Frontiers of Information Technology & Electronic Engineering
www.jzus.zju.edu.cn; engineering.cae.cn; www.springerlink.com
ISSN 2095-9184 (print); ISSN 2095-9230 (online)
E-mail: jzus@zju.edu.cn

Review:

Microwave metamaterials: from exotic physics to novel information systems*

Rui-yuan WU[1,2], Tie-jun CUI[†‡1,2]

[1]*State Key Laboratory of Millimeter Waves, Southeast University, Nanjing 210096, China*

[2]*Synergetic Innovation Center of Wireless Communication Technology, Southeast University, Nanjing 210096, China*

[†]E-mail: tjcui@seu.edu.cn

Received Sept. 2, 2019; Revision accepted Dec. 25, 2019; Crosschecked Jan. 13, 2020

Abstract: Metamaterials and metasurfaces have attracted much attention due to their powerful ability to control electromagnetic (EM) waves. In this paper, we review the recent developments in the field of EM metamaterials, starting from their exotic physics to their applications in novel information systems. First, we show the fundamental understanding on traditional metamaterials based on the effective medium theory and related applications, such as invisibility cloaks and meta-lenses. Second, we review the two-dimensional versions of metamaterials, i.e., metasurfaces, for controlling spatial waves and surface waves and thereafter present their typical designs. In particular, we briefly introduce spoof surface plasmon polaritons and their applications in microwave frequencies. Following the above approach, we emphatically present the concepts of digital coding metamaterials, programmable metamaterials, and information metamaterials. By extending the principles of information science to metamaterial designs, several functional devices and information systems are presented, which enable digital and EM-wave manipulations simultaneously. Finally, we give a brief summary of the development prospects for microwave metamaterials.

Key words: Metamaterial; Effective medium theory; Metasurface; Surface plasmon polaritons; Digital coding; Programmable; Information

https://doi.org/10.1631/FITEE.1900465 **CLC number:** TN99

1 Introduction

From ancient times, controlling electromagnetic (EM) waves has been always an ongoing desire for humans, because it can bring more convenience to human life. Whether using a convex lens to make fire or adopting the periscope for detection activities, Fermat's principle and Snell's law provided the subjective probability of humans using EM waves, but more complicated applications have been restricted by objective conditions, e.g., permittivity ε>1 and permeability μ>1, in almost all natural materials. In the latter half of the 20th century, Veselago (1967) proposed a bold assumption: if ε and μ of a material are both negative, the EM properties would be obviously different from those of conventional materials, even completely opposite. When EM waves propagate in this kind of material, the wave vector $\boldsymbol{k}$, electric field vector $\boldsymbol{E}$, and magnetic field vector $\boldsymbol{H}$ obey the "left-handed law." Hence, this material is also called "left-handed material" and has been predicted to have several unique properties, such as negative

‡ Corresponding author

* Project supported by the National Key Research and Development Program of China (Nos. 2017YFA0700201, 2017YFA0700202, and 2017YFA0700203), the National Natural Science Foundation of China (Nos. 61631007, 61731010, 61735010, 61722106, 61701107, and 61701108), the Fund for International Cooperation and Exchange of the National Natural Science Foundation of China (No. 61761136007), the 111 Project (No. 111-2-05), the Fundamental Research Funds for the Central Universities, the Postgraduate Research & Practice Innovation Program of Jiangsu Province, China (No. KYCX17_0092), and the Scientific Research Foundation of Graduate School of Southeast University, China (No. YBJJ-1815)

ORCID: Rui-yuan WU, https://orcid.org/0000-0002-8318-9800; Tie-jun CUI, https://orcid.org/0000-0002-5862-1497

refraction, inverse Doppler effect, and backward Cherenkov radiation (Veselago, 1967). However, due to the lack of actual design approaches, this concept could not raise much attention until nearly 30 years later. At the end of the 20th century, John PENDRY and his group (Pendry et al., 1996, 1999; Pendry, 2000) proposed effective methods to construct left-handed metamaterials based on the effective medium theory, which were then verified experimentally using artificial structures such as split-ring resonators (SRRs) and metallic wires (Smith et al., 2000; Shelby et al., 2001). Metamaterials exhibit many exotic physical phenomena and enable various applications, including invisibility cloaks, meta-lenses, and super-resolution imaging (Smith et al., 2004; Engheta and Ziolkowski, 2006; Cui et al., 2010; Zheludev and Kivshar, 2012).

However, because of the bulky property of metamaterials, it is difficult to integrate them into systems. Sievenpiper et al. (1999) proposed a mushroom-shaped artificial band-gap structure that exhibits high impedance to control the EM waves. This can be treated as the prototype of the metasurface, which can also be regarded as the two-dimensional (2D) version of a metamaterial (Holloway et al., 2012). Subsequently, Capasso's group proposed the generalized Snell law based on phase or amplitude discontinuities to tailor EM reflection and refraction (Yu NF et al., 2012). They explained that the working scheme of a metasurface is to construct phase or amplitude profiles using proper meta-particles, rather than phase accumulation in space. Hence, metasurfaces are characterized by low quality, low volume, and easy conformability and integration. Due to these advantages, they have attracted considerable attention recently (Chen HT et al., 2016; Zhang L et al., 2016; Ding et al., 2017).

Another special type of metamaterial is related to spoof surface plasmon polaritons (SPPs), inspired by SPPs in the optical frequencies. Optical SPPs possess many significant features, such as field enhancement and wavelength compression. However, it is hard to transmit SPP waves at optical frequencies due to huge losses. With the help of metamaterials, it is possible to mimic the spoof SPP effect in the microwave and terahertz regions. Pendry et al. (2004) first proposed a three-dimensional (3D) artificial structure to create an SPP-like performance by drilling an array of subwavelength holes in a metallic block; other 3D structures such as silicon prisms were also found to excite SPPs (Pendry et al., 2004; O'Hara et al., 2005). These structures were then enhanced to 2D ultrathin structures with conformal property to guide the SPP waves flexibly (Shen XP et al., 2013). Because of their exotic features, SPPs can be treated as novel EM transmission lines and can be widely used in microwave devices and systems (Gao Z et al., 2018; Tang et al., 2019).

The above-mentioned metamaterials or metasurfaces can be classified as "analog metamaterials" because of the continual manipulations on EM coefficients regardless of the effective refraction indexes or phase and amplitude. Following the trend of information science, Giovampaola and Engheta (2014) and Cui et al. (2014) independently proposed the concept of digital metamaterials. In contrast to conventional metamaterials, the EM characteristics were presented through several discrete digital states in coding and digital metamaterials (Cui et al., 2014). For example, there are two binary digits "0" and "1" in 1-bit coding metamaterials, and the phase responses of the corresponding coding particles are 0° and 180°, respectively (Cui et al., 2014). Actually, the phase difference between the coding particles, rather than the absolute phase, is an important value in EM manipulation. Therefore, this scheme can be easily extended to the 2-bit case and cases with more bits. Because the property of the coding particle no longer relies on the continuous effective medium theory or phase shift, the near- or far-field radiations of coding and digital metamaterials depend on the coding sequences or coding patterns, wherein digital information is directly involved. Furthermore, Cui et al. (2014) created programmable metamaterials by loading active devices on the coding particles to achieve real-time manipulations on EM information. Hence, coding, digital, and programmable metamaterials build the bridge between information science and physical metamaterials, and they can be promoted to information metamaterials to accomplish more information-driven manipulations on EM waves and future information systems (Cui et al., 2017a; Cui, 2017, 2018; Fu and Cui, 2019; Li LL and Cui, 2019).

In the following sections, we review the recent progress on metamaterials from two aspects, i.e., the

exotic physics displayed by the traditional effective medium metamaterials, metasurfaces, and spoof SPPs, and the functional devices and novel systems enabled by the information metamaterials (including coding, digital, and programmable metamaterials).

2 Analog metamaterials

2.1 Effective medium metamaterials

In contrast to the natural materials consisting of molecules and atoms, metamaterials are actually composed of subwavelength-scale meta-particles arranged periodically or quasi-periodically. The major difference between metamaterials and other earlier periodic structures such as photonic band-gap structures and frequency selective surfaces is the smaller particle size, which avoids the mutual coupling of adjacent particles. Smith et al. (2000) constructed a composite medium using a periodic array of conducting nonmagnetic SRRs and continuous wires, and experimentally demonstrated the feasibility of simultaneous negative permittivity and permeability, the most prominent characteristic of left-handed metamaterials. The earlier metamaterial designs follow the effective medium mechanism based on Lorentz–Drude models. Thus, metamaterials can be described by continuous effective medium parameters (effective permittivity ε and effective permeability μ), which can be obtained from simulated or experimentally measured scatter parameters (S-parameters). Because the effective EM coefficients of each particle can be controlled independently and arbitrarily, the total metamaterial can exhibit some exotic characteristics that cannot be achieved in nature, such as negative refraction (Padilla et al., 2006) and even zero refraction (Moitra et al., 2013).

This approach can only clearly provide the physical features, but is inaccurate in determining the effective medium parameters quantitatively. Therefore, Liu RP et al. (2007) developed a general model of effective media and established the relationship between meta-particles and the entire metamaterial. Accordingly, the average permittivity and permeability can be defined because the size of the meta-particle is in subwavelength scale and a discrete form of Maxwell's equations on the macroscale is also obtained. Hence, the effective parameters of the artificial metamaterial sample composed of periodic particles can be expressed as follows:

$$\varepsilon_{\text{eff}}=\overline{\varepsilon}\frac{\theta/2}{\sin(\theta/2)}\left[\cos(\theta/2)\right]^{-S_{\text{b}}}, \tag{1}$$

$$\mu_{\text{eff}}=\overline{\mu}\frac{\theta/2}{\sin(\theta/2)}\left[\cos(\theta/2)\right]^{S_{\text{b}}}, \tag{2}$$

in which ε_{eff} and μ_{eff} are the required effective permittivity and permeability, respectively, $\overline{\varepsilon}$ and $\overline{\mu}$ represent the average permittivity and permeability, respectively, θ indicates the phase shift of one particle, S_{b}=1 for the average electric field, and S_{b}=−1 for the average magnetic field (Liu RP et al., 2007).

Based on this theory, the effective parameters of meta-particles can be accurately retrieved and predicted, rapidly from the numerical scattering parameter and the available wave modes (including the propagation mode, pure plasma mode, and resonant crystal band-gap mode). Figs. 1a–1c and Figs. 1d–1f show the retrieved permittivity and permeability of the SRR structure and electric-LC (ELC) structure, respectively. The agreement with theoretical results demonstrates the validity of the proposed retrieval approach. This provides the possibility for the fast design of the next large-scale metamaterial system and even the fully automatic procedure (Liu RP et al., 2007).

Combining the effective medium theory with several optical principles, a series of exotic physical phenomena of the metamaterials have emerged and attracted much attention. Pendry et al. (2006) proposed an approach to control EM waves artificially, laying the theoretical foundation for the famous EM invisibility cloak. Different from the ordinary materials in nature, metamaterials can easily present electromagnetically inhomogeneous effective permittivity and permeability distribution in the cloak calculated by the ray tracing approach and transformation optics, enabling unusually distorted EM propagation; thus, EM waves can bypass the inner target. This concept was soon experimentally demonstrated at microwave frequencies by Smith's group (Schurig et al., 2006). A ring-shaped array of SRR structures formed an effective cloak and the inner object was perfectly "hidden" (Schurig et al., 2006). This work verified the possibility of

metamaterial invisible cloaks and was selected as one of the 10 scientific breakthroughs of *Science* in 2006.

However, there were still some drawbacks, such as narrow operating band and high loss, which limit more applications. Hence, a 2D broadband ground-plane invisibility cloak using non-resonant I-shaped meta-particles was proposed (Liu R et al., 2009). The relative refraction index was controlled by the size of the I-shaped structure. By arranging the structures with different sizes according to a predesigned refraction-index profile, it was ensured that the inner target had little influence on the reflecting EM field and thus it would not be detected by the incident waves, illustrating good invisible performance from 13 to 16 GHz, compared with the ideal situation.

Later, a 3D fully dielectric invisibility cloak was completed by Ma HF and Cui (2010a) by adopting bulky drilled-hole meta-particles (Fig. 1g). The effective refraction index of the meta-particle depends on the thickness and diameter of the hole. As in the simulated performance (Fig. 1h), the field distributions with a cloak are very similar to that of only flat ground, implying that good cloaking effects are achieved using this 3D cloak in a wide-frequency band for parallel polarization (Ma HF and Cui, 2010a). Because metamaterial cloaks have great potential in modern military, even now, the metamaterial cloak is being further developed with more elaborate ideas (Chen HS et al., 2007; Landy and Smith, 2013; Park et al., 2019).

Another important research area on metamaterials is the high-performance meta-lens (Lin et al., 2008; Kundtz and Smith, 2010; Ma HF and Cui, 2010b; Jiang et al., 2016). With the help of

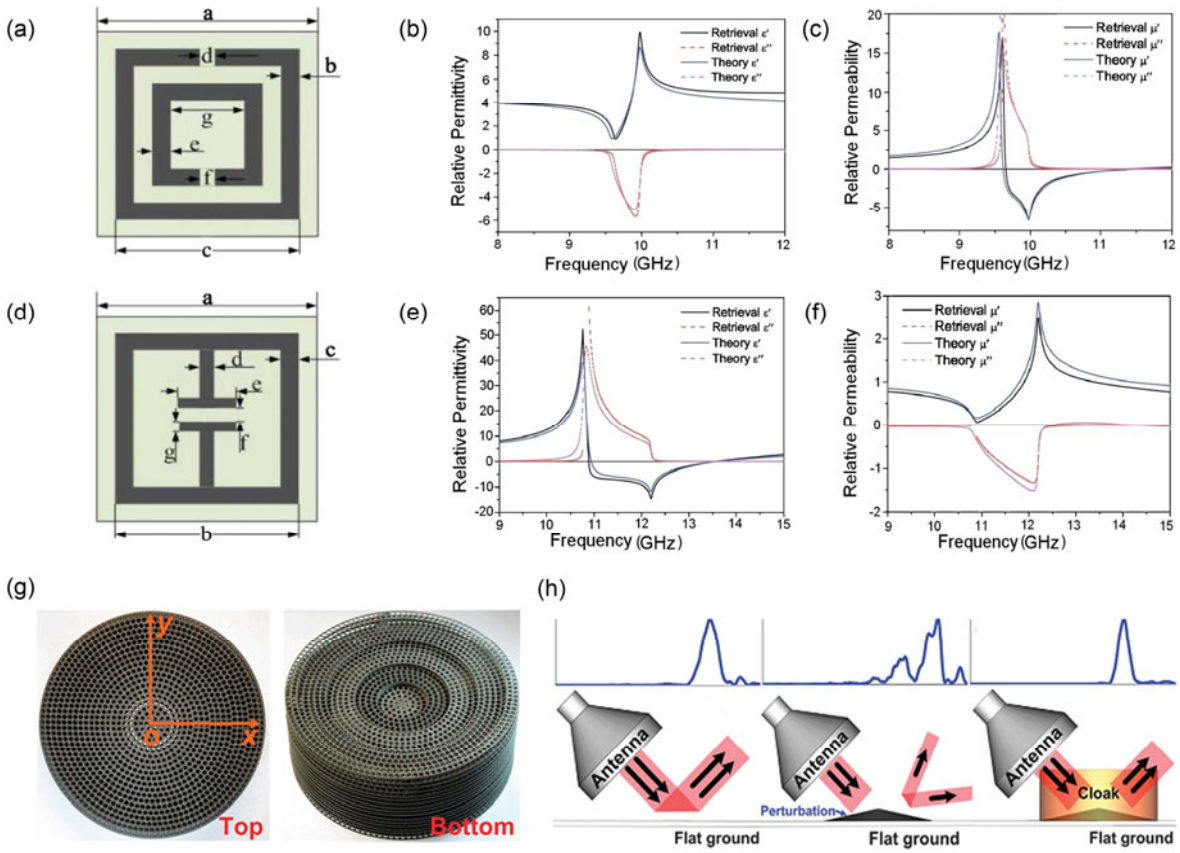

Fig. 1 Metamaterials effective parameter retrieval and cloaks

(a–c) Retrieved permittivity and permeability of the split-ring resonator (SRR) structure; (d–f) Retrieved permittivity and permeability of the electric-LC (ELC) structure; (g) 3D fully dielectric invisibility cloak by the bulky drilled-hole particles; (h) Working situations for measurements and simulations and the predicted far-field patterns. (a)–(f) are reprinted from Liu RP et al. (2007), Copyright 2007, with permission from the American Physical Society; (g) and (h) are reprinted from Ma HF and Cui (2010a), Copyright 2010, with permission from Springer Nature, licensed under CC-BY-NC-SA-3.0

gradient-refractive-index (GRIN) metamaterials, a 3D broadband and broad-angle Luneburg lens with a flattened focal surface was achieved at microwave frequencies (Ma HF and Cui, 2010b). The complete meta-lens consisted of an assembly of three sub-parts composed of three types of drilled-hole particles of different volumes (Fig. 2a); thus, the available range of the effective refraction index in each part can be inhomogeneous. Using transformation optics to calculate the effective refractive index distribution, an approximation enabled the creation of the 3D Luneburg lens using isotropic dielectric materials. Fig. 2b illustrates the outstanding measured beam-scanning results of the near electric fields outside the lens at 12.5, 15, and 18 GHz with different offset distances of 0, 10, and 30 mm from the center of the focal plane, respectively. This design exhibits several advantages such as high gain, low side lobes, large radiation angles, and broad working band, indicating very promising prospects in antenna applications (Chen X et al., 2011; Qi et al., 2013; Ramaccia et al., 2013). A typical example is a metamaterial-loaded lens antenna for emitting planar EM waves assisted by geometrical optics (Fig. 2c). The proposed design showed good performance with high gain and low side lobes from 8 to 12.5 GHz, as shown in Figs. 2d and 2e (Chen X et al., 2011). Other meaningful applications, such as EM black holes (Narimanov and Kildishev, 2009; Cheng et al., 2010), absorbers (Sun JB et al., 2011; Huang et al., 2013), filters (Gil et al., 2008), and polarization converters (Markovich et al., 2013), can also be fulfilled by metamaterials, verifying their prominent EM manipulating ability.

2.2 Metasurfaces: 2D version of metamaterials

The principle of EM manipulation by metamaterials with 3D structures is the spatial phase accumulation along the propagating direction, so the thickness will be relatively large compared with the wavelength. This process may face several difficulties

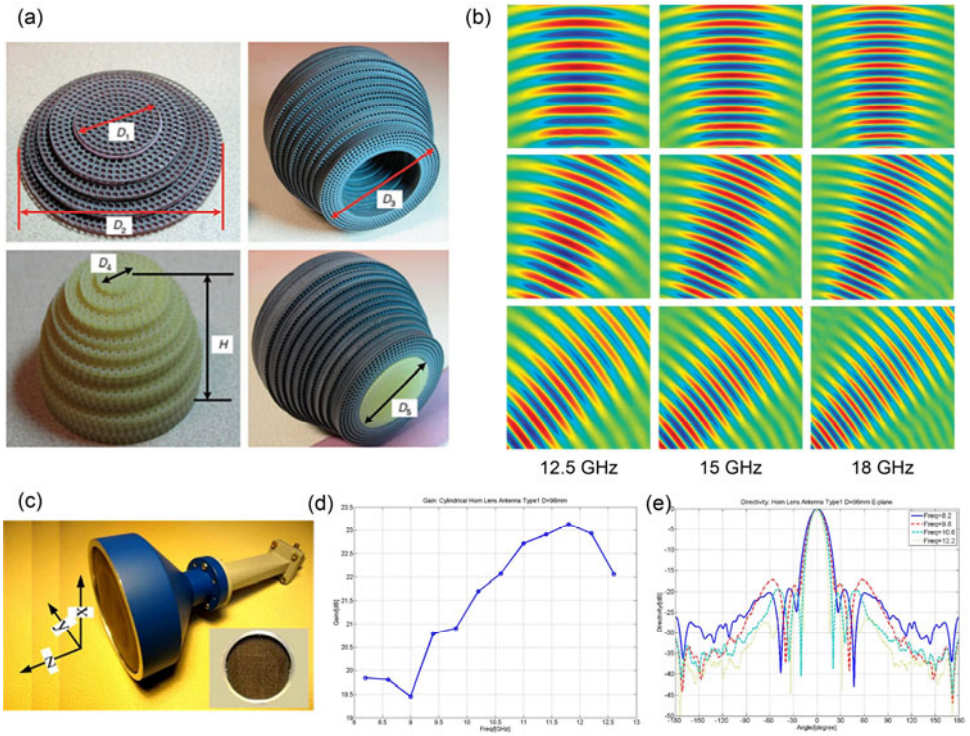

Fig. 2 Gradient-refractive-index (GRIN) metamaterial lens and lens antennas

(a) Construction of the 3D metamaterial Luneburg lens (the three parts are composed of different types of drilled-hole particles with different effective refractive indexes and finally assembled together); (b) Experimental beam-scanning results of near-field electric fields outside the lens at 12.5, 15, and 18 GHz with different offset distances 0, 10, and 30 mm from the center of the focal plane, respectively; (c) Photograph of the lens antenna setup that can radiate planar EM waves; (d, e) Measured gain and E-plane far-field radiating patterns. (a) and (b) are reprinted from Ma HF and Cui (2010b), Copyright 2010, with permission from Springer Nature; (c)–(e) are reprinted from Chen X et al. (2011), Copyright 2011, with permission from AIP Publishing

in fabrications and integrations, especially in terahertz and optical frequencies. Sievenpiper et al. (1999) proposed a 2D EM band-gap structure, which can be regarded as the beginning of the 2D metamaterial, termed metasurface. This kind of mushroom-shaped metasurfaces with high impedance has been widely used in antennas and other EM devices to reduce the size and profile (Sievenpiper et al., 1999). During the earlier time, the generalized sheet transition condition method (Kuester et al., 2003) and transverse resonance method (Collin, 1960) were first presented to analyze the EM performance of metasurfaces. Then, Capasso's group proposed the generalized Snell law for metasurfaces (Yu NF et al., 2012), opening the ceremony for rapid developments. Phase discontinuities between neighboring particles on the metasurfaces were designed artificially to manipulate EM waves, rather than for space accumulation as in 3D metamaterials. For example, when the gradient phase discontinuities were implemented by V-shaped structures, the incident wave would be bent to an oblique transmitting direction (Yu NF et al., 2012). Therefore, metasurfaces possess a series of advantages of brief design, low cost, small weight, and easy integration.

Because metasurfaces are formed by a flat array of planar subwavelength meta-particles, we can adjust the phase discontinuities constructed by the particles with different geometries to manipulate reflecting/transmitting EM waves according to the predesigned phase distributions (Li Y et al., 2013; Wei et al., 2013; Shalaev et al., 2015). The incident EM waves are tailored accordingly, showing the corresponding radiating patterns in the far field. There are two conditions for the basic manipulations on scattering waves, i.e., high amplitude and 360° phase-shifting range. For the reflection-type designs, there is always a metallic ground plate at the bottom of the particle; thus, the reflecting amplitude can be ensured to be of 0 dB, and all the geometrical changes are aimed to adjust the phase shift (Li Y et al., 2013). However, for transmission-type designs, the amplitude should be high enough during the tuning of the transmitting phases; hence, multiple layers of the same or different types are needed to satisfy these two extreme conditions (Wei et al., 2013; Shalaev et al., 2015). In 2013, the Huygens metasurface was proposed to provide bizarre control of EM transmitting properties across electrically thin layers with very low reflections because of the simultaneous generation of electric and magnetic polarization currents (Pfeiffer and Grbic, 2013; Chen K et al., 2017; Wong and Eleftheriades, 2018). The electric and magnetic sheet reactances were induced in the capacitively and inductively loaded traces on the top layer and the capacitively loaded loops on the bottom layer, respectively, controlling the electric sheet admittance and magnetic sheet impedance (Pfeiffer and Grbic, 2013). The major feature of the Huygens metasurface is the highly efficient EM manipulations, demonstrated by the deflecting refraction with 86% efficiency.

Furthermore, more complicated wave-front shaping can be tailored by metasurfaces. Vortex beams, namely, beams with orbital angular momentum (OAM), have attracted much attention recently because they can enlarge the information capacity compared with traditional planar EM waves. The traditional methods to achieve OAM beams include the spiral phase plate and antenna arrays. Now, metasurfaces bring an easy and efficient approach to generate OAM beams by etching the spiral phase distribution on the aperture (Karimi et al., 2014; Yi et al., 2014; Chen MLN et al., 2016; Yu SX et al., 2016a, 2016b, 2016c; Han et al., 2018). The number of OAM modes depends on the integral multiples of 2π in one spiral phase period on the metasurface, and the rotating direction of the spiral distribution determines whether the OAM is positive or negative.

Additionally, surface-wave manipulation is a significant functionality of metasurfaces (Sun SL et al., 2012). Surface-wave lens or leaky-wave radiations can be achieved by controlling the dispersion properties and surface impedance of the particle (Fig. 3a) (Li YB et al., 2014, 2016a; Cai et al., 2015). Fig. 3b illustrates two dual-functional holographic leaky-wave metasurfaces that enable two radiating beams with different polarizations in the same direction and two orthogonal directions, respectively. Besides, this design can achieve frequency-dependent beam-scanning effects with a broad working band and corresponding wide angle-scanning range, as shown in Figs. 3c and 3d (Li YB et al., 2016a).

Recently, multi-coefficient controlled metasurfaces have attracted increasing attention. The key issue involved in the simultaneous manipulations on multiple EM properties is that mutual interference

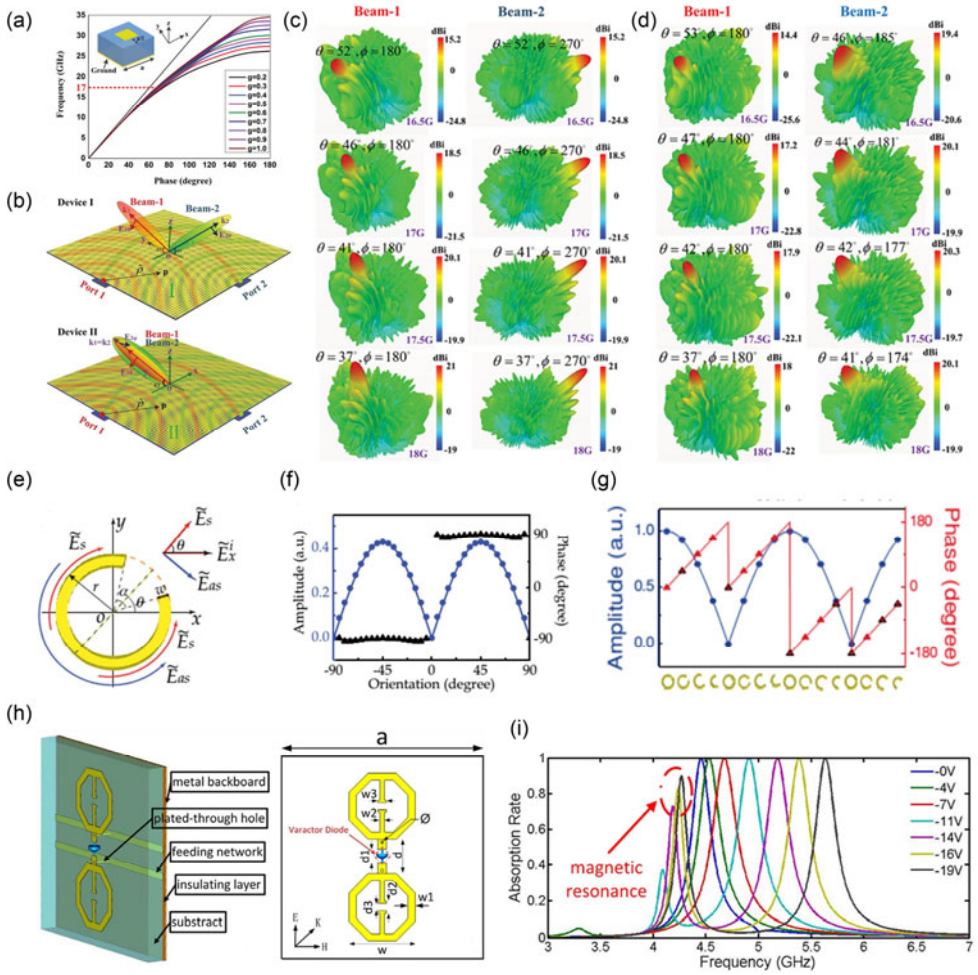

Fig. 3 Dispersion curves of the particle (inset) for leaky-wave metasurfaces (a), schematics of two dual-functional holographic leaky-wave metasurfaces for manipulating surface EM waves and then radiating them (b), full-wave simulation results of devices (I) and (II) respectively (two single beams scanning with frequency from 16.5 to 18 GHz at the same or different azimuth angles) (c, d), sketch and performance of amplitude-phase controllable C-shaped particle respectively (e, f), amplitude and phase profiles of first- and third-order diffractions caused by the particles with different orientations and opening angles (g), structure of an active metamaterial particle absorber (h), and simulation results of absorption rates at different bias voltages (i)

(a)–(d) are reprinted from Li YB et al. (2016a), Copyright 2015, with permission from WILEY-VCH Verlag GmbH & Co. KGaA, Weinheim; (e)–(g) are reprinted from Liu LX et al. (2014), Copyright 2014, with permission from WILEY-VCH Verlag GmbH & Co. KGaA, Weinheim; (h) and (i) are reprinted from Zhao et al. (2013), Copyright 2013, with permission from the authors, licensed under CC BY-3.0

should be avoided. Minatti et al. (2012), Wan et al. (2014), and Xu J et al. (2018) proposed the anisotropic metasurface design to achieve two totally different functionalities differentiated by the polarization of incident waves. The phase responses of the anisotropic meta-particle under different linear or circular polarizations were independently tuned using the corresponding geometrical parameters. Similarly, dual- or multi-band metasurfaces (Li K et al., 2015; Li ZC et al., 2016; Li HP et al., 2018) illustrate their multi-functional potential, but the switching is implemented by changing the working frequency. As we all know, the amplitude- and phase-controllable metasurface is the most difficult to design; thus, examples are rarely seen (Liu LX et al., 2014; Wan et al., 2016b; Xu HX et al., 2019). Liu LX et al. (2014) proposed an original path based on the C-shaped structure (Fig. 3e), and the transmitting amplitude and

phase responses could be manipulated using the orientations and opening angles of the structure (Fig. 3f). By elaborately setting the amplitude and phase profiles, the proposed metasurface can form the power distribution of the diffraction with different orders; Fig. 3g shows a specific profile of first- and third-order diffractions.

Furthermore, using the huge amplitude change brought in by resonance of the metasurface, reflection-type or transmission-type ultrathin metasurface absorbers have been created (Wakatsuchi et al., 2013; Zhao et al., 2013; Liu S et al., 2015; Li Y and Assouar, 2016). A typical design in terahertz frequencies used 12 differently sized metallic bars on three polyimide layers with the same spacing to design a broadband absorber. The measured absorption exceeded 90%, from 0.81 to 1.32 THz (Liu S et al., 2015). Moreover, by loading active devices on the meta-particle (Fig. 3h), the working frequency can be tuned by changing the bias voltage without affecting the high absorption rate (Fig. 3i) (Zhao et al., 2013). Moreover, metasurfaces provide approaches for constructing ultrathin polarization converters for both linear and circular polarizations (Gao X et al., 2015; Li ZC et al., 2015; Wu PC et al., 2017). These prominent features make the future of metasurfaces even brighter in actual applications.

2.3 Spoof SPPs

Spoof SPPs are another kind of widely investigated metamaterial, providing a totally neoteric approach to manipulate EM waves in microwave regimes. SPPs are highly localized EM waves that usually emerge on the interface of two media with opposite permittivities but only in optical frequencies. However, it is impossible to achieve SPPs in microwave bands because metallic materials such as gold and copper behave as good conductors without negative permittivity. Hence, researchers used the artificial metamaterial structures such as 2D periodic arrays of sub-wavelength grooves, holes, dimples, or 3D wires with grooves, to mimic high localization and dispersion characteristics as spoof SPPs in the microwave region. Pendry et al. (2004) proposed a specific design of spoof SPPs to control the dispersion property. A perfect conductor with an array of piercing square holes efficiently confined the incident waves on the interface, showing exponential decay along the z direction, which is similar to the performances of natural SPPs (Pendry et al., 2004; Garcia-Vidal et al., 2005). However, such structures need to suffer from some disadvantages, such as difficulties in fabrication, integration, and conformability.

In 2013, a free-standing planar plasmonic metamaterial was proposed to solve these problems (Shen XP and Cui, 2013; Shen XP et al., 2013). The structure was constructed on a thin metal film with an etched periodic array of grooves on its edge (Fig. 4a) to excite the spoof SPPs and propagate them along the structure. Because the film's thickness was nearly zero, it could be arbitrarily distorted or bent, even divided between two separate paths in 2D and 3D conditions (Fig. 4b). To construct conformal surface plasmons, the confined spoof SPPs can propagate along the corrugated metallic strip (Shen XP et al., 2013).

These excellent characteristics make the spoof SPPs more attractive, and several applications emerge such as SPP transmission lines and other SPP devices. However, another important issue concerns how to feed the SPP transmission lines. Different form 3D metamaterials or metasurfaces, which can easily convert spatial waves to surface waves, transmission lines are always integrated in the microwave devices or systems; thus, SPP transmission lines should be fed similar to the method for traditional designs such as microstrips and coplanar waveguides (CPWs). Ma HF et al. (2014) smoothly converted the guided wave from the conventional CPW to spoof SPPs in an ultrathin corrugated metallic strip with high efficiency in a wide working band. To deal with the mismatching in momentum and impedance between the CPW and SPP transmission lines, matching transitions with gradient grooves and flaring ground were arranged in both symmetrical strips (Fig. 4c). As shown in Fig. 4d, the 2D simulated and measured e-field distributions clearly prove that SPPs are smoothly converted from the guided waves in CPW, and high efficiency was demonstrated by the results of the S-parameters with and without matching transition (Fig. 4e). This design opens up a string of conversion devices of SPP and traditional planar waveguides in the microwave band, and several following designs show more converting schemes (Liao et al., 2014). Furthermore, common instruments such as filters, couplers, and power dividers, can be designed by SPP

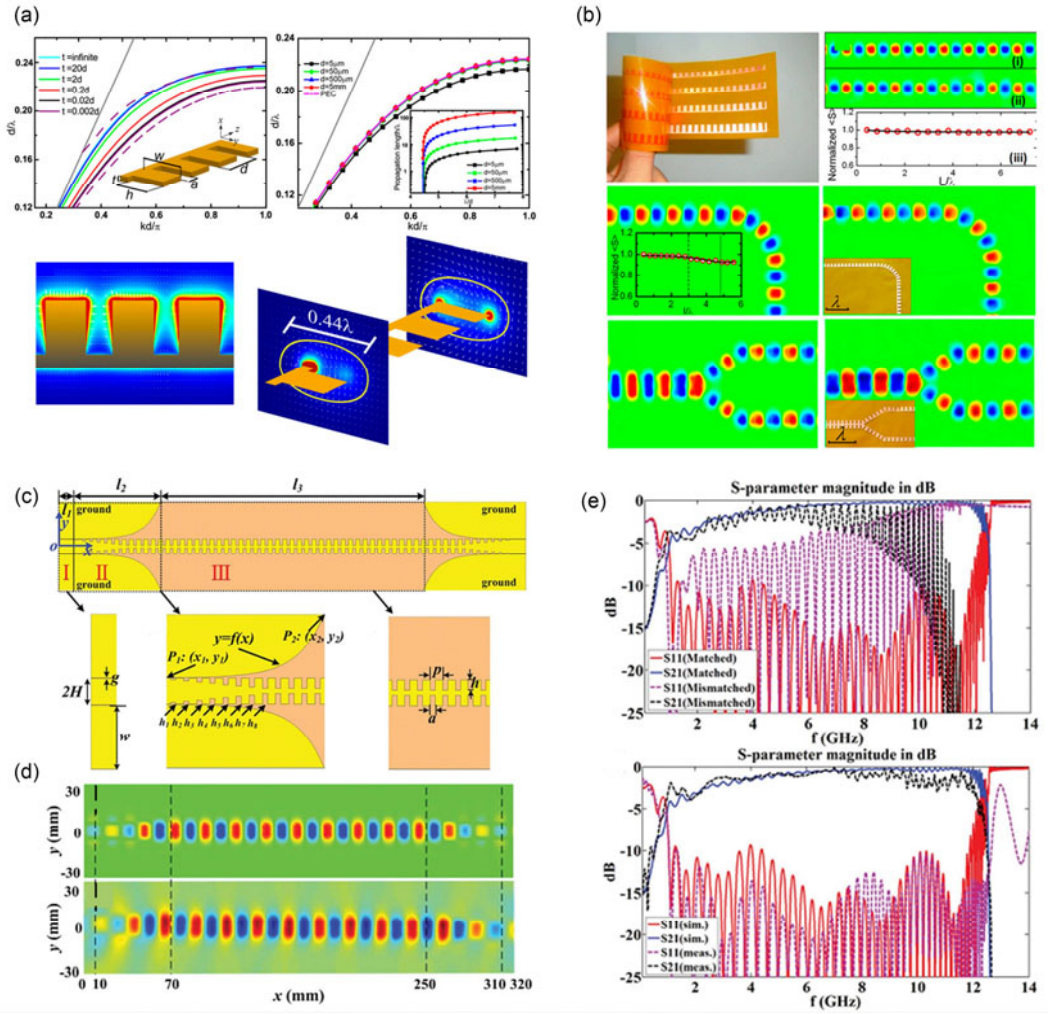

Fig. 4 Sketch and performance of the flexible surface plasmon polariton (SPP) constructed on a thin metal film with an etched periodic array of grooves on its edge (a), simulation and measurement results of the conformal SPP to guide waves arbitrarily (b), configuration to convert CPWs to SPP waves (the highlight is the matching transition with gradient grooves and flaring ground) (c), 2D simulated and measured e-field distributions of the proposed hybrid waveguide (d), and simulation and measurement results of the proposed hybrid waveguide with and without the matching transition (e)

(a) and (b) are reprinted from Shen XP et al. (2013), Copyright 2013, with permission from the National Academy of Sciences; (c)–(e) are reprinted from Ma HF et al. (2014), Copyright 2013, with permission from WILEY-VCH Verlag GmbH & Co. KGaA, Weinheim

transmission lines (Liu XY et al., 2016; Zhang Q et al., 2016; Wang ZX et al., 2018). In addition, active devices such as semiconductor chips have been integrated in SPP structures to achieve SPP frequency multiplier and amplifier, respectively (Zhang HC et al., 2015a, 2015b; Zhang XR et al., 2018).

We can also convert the SPP waves to spatial waves and radiate them by designing non-uniform corrugated structures that can also be called plasmonic emitters (Kong et al., 2016; Yin et al., 2016; Wang M et al., 2018). In 2016, a typical design of a radiating SPP waveguide was proposed, which was also fed by CPW, but the metallic strip showed a sinuous shape with several modulation periods (Kong et al., 2016). The radiating beam can scan continuously as the frequency varies. Furthermore, to increase the radiation efficiency of the SPP waveguide at the broadside, an asymmetrical design was further presented to reduce the reflections (Kong et al., 2016). This has also been promoted to active cases and

enjoys more manipulating freedom (Wang M et al., 2018).

3 Digital information metamaterials

3.1 Introduction to coding and digital metamaterials

As mentioned earlier, the basic EM information of the metamaterial and metasurface is effective coefficients or phase and amplitude discontinuities. Hence, due to the continual manipulations of EM waves, they are regarded as "analog metamaterials." Now, information technology plays a major role in daily life and engineering, which limits the application of conventional metamaterials in integrated systems because of the matching transition working principle. Thus, it would be a big progress if metamaterials are digitally described and incorporated in digital information systems. In 2014, Engheta's group from University of Pennsylvania (Giovampaola and Engheta, 2014) and Cui's group from Southeast University (Cui et al., 2014) independently proposed the concept of digital metamaterials, which could be treated as the ancestor of information metamaterials.

Giovampaola and Engheta (2014) constructed binary metamaterials from the effective medium theory and adopted two numerical representations, "0" and "1," to describe the effective permittivity in two different cases. The excellent performances of digital metamaterials agreed well with those of traditional homogeneous metamaterials, proving that influence by discretization can be ignored. This novel concept introduces a simple but powerful approach for researchers to build metamaterial devices and systems.

At the same time, Cui et al. (2014) proposed the concept of coding and digital metamaterials inspired by the information science beyond the traditional effective medium theory. Although the properties of metamaterials are similar in the digital state, the intrinsic implications of each coding particle here are derived from the reflecting or transmitting phase (or amplitude) instead of permittivity (Cui et al., 2014). Hence, the incident EM waves can be tailored digitally by establishing different coding sequences or patterns. Specifically, 1-bit coding metamaterials contain two digital states, "0" and "1," denoting phase responses 0° and 180°, respectively, as shown in Fig. 5a (Cui et al., 2014). It should be highlighted that the required phase response is actually the phase difference between the two coding particles, rather than the absolute phases. This scheme can be easily extended to multi-bit coding metamaterials. For example, Fig. 5b displays the 2-bit coding, which includes four types of digits, 00, 01, 10, and 11 (they can be written as 0, 1, 2, and 3 for simplicity in further operations), corresponding to the phase responses as 0°, 90°, 180°, and 270°, respectively (Cui et al., 2014). The desired phase responses can be achieved through tuning of the geometrical sizes of the metallic patch or other structures.

Hence, the functions of coding metamaterials/metasurfaces depend on the coding sequences or coding patterns, composed of periodically or non-periodically arranged digital states. Fig. 5c shows the radiating patterns of 000000…/000000..., 010101…/010101..., and 010101…/101010..., where the EM radiation retains a pencil beam or splits it to dual or four symmetrical beams. Generally, the larger the bit number of coding digits, the higher the precision and complexity of EM manipulations. For example, if the coding sequence is "01230123…" along the x direction (Fig. 5d), the far-field radiating pattern is a single oblique beam with the deflecting angle calculated as follows (Cui et al., 2014):

$$\theta=\arcsin(\lambda/\Gamma), \tag{3}$$

in which λ is the working wavelength and Γ is the period of the coding sequence. However, sometimes designing a well-performing unit is not an easy task, especially for the multi-bit cases. Zhang Q et al. (2017, 2019) proposed a software-automatically-designed approach to establish the fully digital procedure for assembly from meta-particle to metasurface. Figs. 5e–5h show a series of 2-bit coding particles achieved by software-automatically-designed approaches. Combined with the commercial EM software, even 4-bit coding particles can be achieved rapidly by optimizing the arrangement of the micro-coding units and then assembling them together to tailor outgoing EM waves flexibly.

Several pioneering coding designs have been achieved based on the different EM properties. Liu S et al. (2016a) proposed an ultrathin and flexible polarization-dependent 1- and 2-bit anisotropic

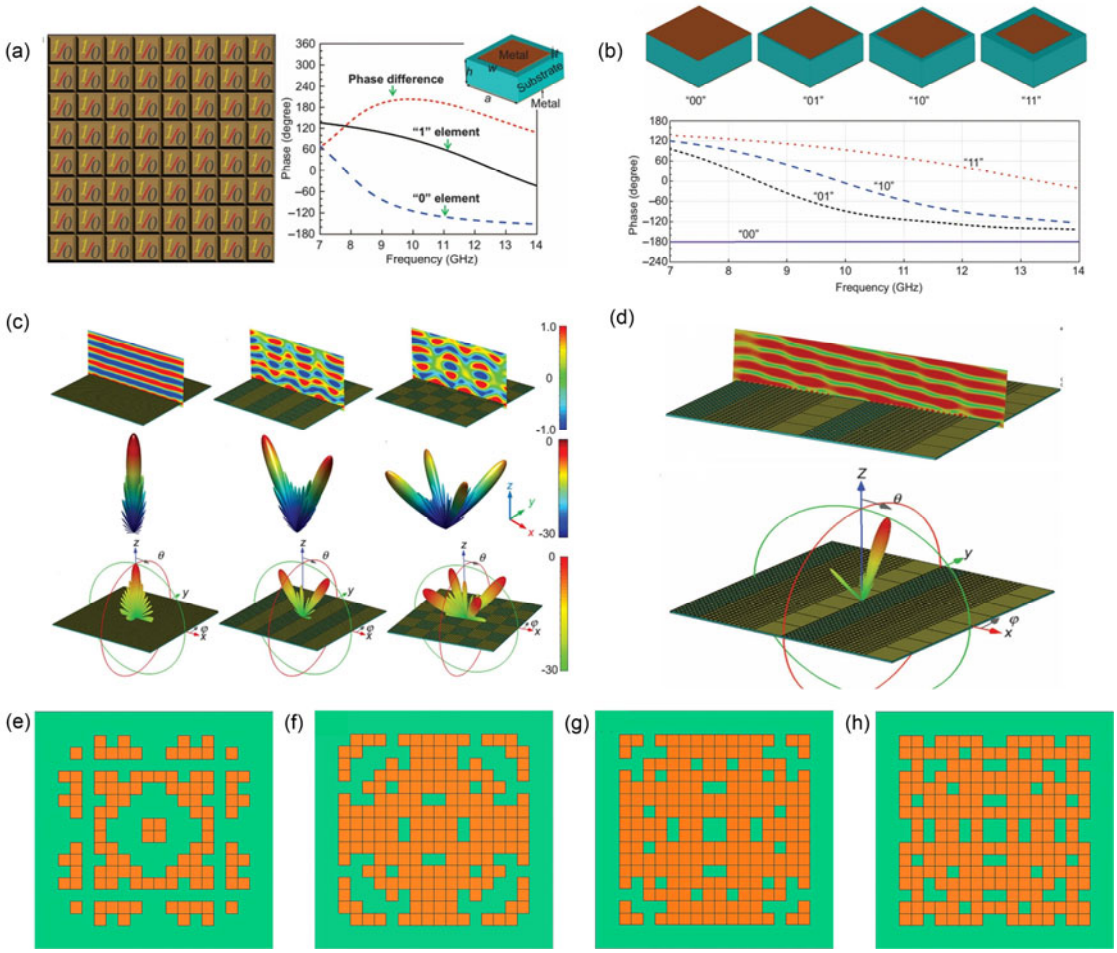

Fig. 5 Working principle of 1-bit coding and digital metasurface and a specific 1-bit coding particle (a), 2-bit coding particles and corresponding phase responses (b), simulated near- and far-field radiating patterns of three different coding patterns (000000…/000000..., 010101…/010101..., and 010101…/101010...) (c), single deflecting beam achieved by 2-bit coding sequence 01230123… (d), and 2-bit coding particles achieved by software-automatically-designed approaches (e–h)

(a)–(d) are reprinted from Cui et al. (2014), Copyright 2014, with permission from Springer Nature, licensed under CC-BY-NC-SA-3.0; (e)–(h) are reprinted from Zhang Q et al. (2017), Copyright 2017, with permission from Springer Nature, licensed under CC BY-4.0

coding metasurface at terahertz frequencies (Fig. 6a). The coding particles independently displayed different digital states at different polarizations (Fig. 6b). By elaborately designing coding patterns for *x*- and *y*-polarized EM waves on the shared aperture simultaneously, the corresponding outgoing waves can be anomalously reflected or independently diffused in three dimensions (Liu S et al., 2016a). Furthermore, Liu S et al. (2016c) and Bai et al. (2018) proposed the dual- and tri-band coding metamaterials, respectively, which could perform different reflecting digital states at different frequencies independently (Figs. 6c and 6d). Such multiple functions at different polarizations or frequencies can be directly used as a beam splitter and may find applications in more potential EM systems. Then, the multi-band designs are extended to frequency coding metamaterials by introducing frequency sensitivities to exhibit various coding sequences with the tuning of the working frequency. By employing four different coding particles, the radiating performance is changed from single beam to dual beams or four beams with the coding pattern from 000000…/000000… to 010101…/010101… or 010101…/101010… (Wu HT et al., 2017).

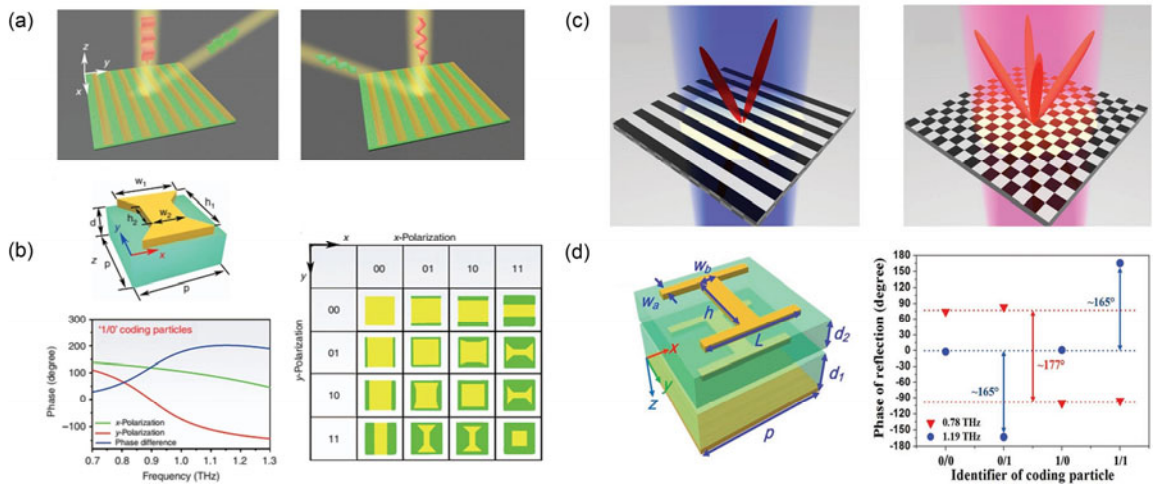

Fig. 6 Working scheme of anisotropic coding and digital metasurfaces (the *x*- and *y*-polarized EM incident waves will be bent in different directions) (a), 1- and 2-bit anisotropic coding particles (b), working scheme of dual-band coding and digital metasurfaces (the EM incidence at different working frequencies will show different functionalities) (c), and 2-bit dual-band coding particles (d)

(a) and (b) are reprinted from Liu S et al. (2016a), Copyright 2016, with permission from Springer Nature, licensed under CC-BY-NC-SA-4.0; (c) and (d) are reprinted from Liu S et al. (2016c), Copyright 2016, with permission from WILEY-VCH Verlag GmbH & Co. KGaA, Weinheim

When the coding patterns are in gradient or chessboard cases, they can achieve only several typical radiating performances. If we want to achieve more complicated functions, it is hard to directly design corresponding coding patterns without optimizations. To solve this problem, the convolution operation (Liu S et al., 2016b) and addition theorem (Wu RY et al., 2018) were proposed to obtain more complicated radiating patterns. Convolution operation is derived from the Fourier transformation between coding patterns and far-field radiating patterns (Liu S et al., 2016b). Hence, the properties in Fourier transformation can be implemented in the coding pattern designs. As shown in Fig. 7a, the scattering-pattern shift, namely, the initial radiating pattern constructed by the cross-shaped coding pattern being shifted to an oblique direction caused by the gradient coding pattern, is analogous to the shift in frequency spectra caused by the convolution operation (Liu S et al., 2016b). For example, Fig. 7b shows a procedure to deflect the dual-beam radiation produced by 2-bit pattern 020202… through the convolution operation with another gradient coding sequence 01230123…. Additionally, this approach breaks through the limitation of the deflecting angle from Eq. (3), and the angle can theoretically have arbitrary values through several times of convolution. Thus, the addition theorem starts from the basic EM theorem and introduces the concept of complex codes, which involve all the complex phase parts $e^{j\varphi}$ (Wu RY et al., 2018). Hence, the addition of these codes obeys the regulations related to complex numbers. On the unit-cell level, the addition theorem reveals the inherent relationship among different coding scales; on the metasurface-system level, it means superposition of two coding patterns, implying that two far-field scattering patterns will appear simultaneously on the shared aperture (Figs. 7c and 7d) (Wu RY et al., 2018). These two methods lay the foundation of achieving more flexible and complicated manipulations on both near- and far-field EM information (Cui et al., 2017b; Bie et al., 2018; Jing et al., 2018).

3.2 Functional applications of coding and digital metamaterials

Coding and digital metamaterials find many applications in both microwave and terahertz regions. Even at acoustic frequencies, they can control acoustic waves digitally with high efficiency (Xie et al., 2017; Bai et al., 2019; Zhang C et al., 2019). The most common application is the manipulation on the far-field beam. The radiating beams can be controlled digitally by the corresponding coding patterns, such as multiple beams and asymmetrical beams (Shen Z

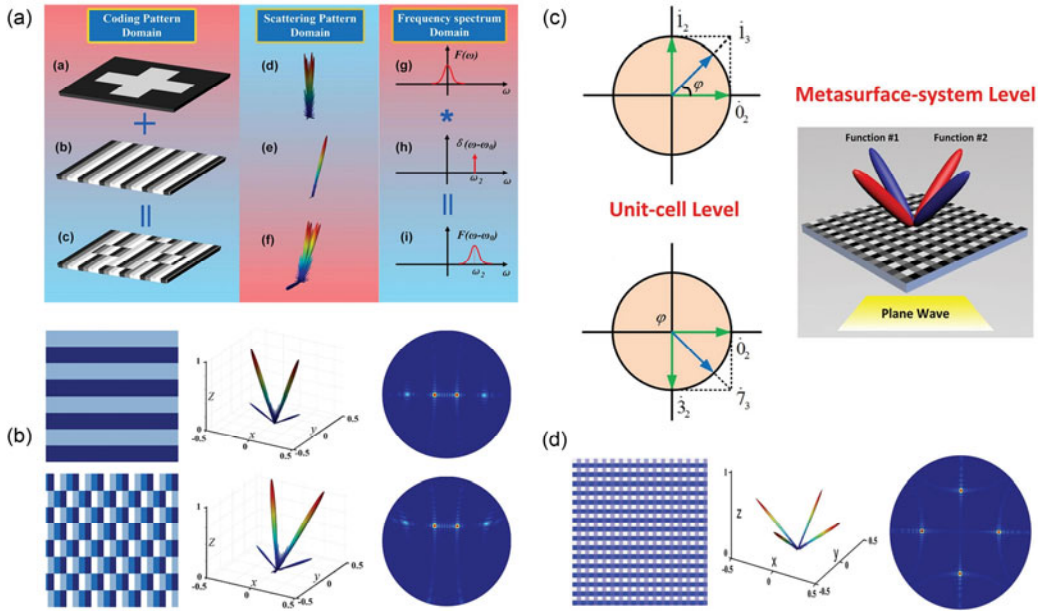

Fig. 7 Schematic illustration of the principle of convolution operations, providing a brief method to shift the beam digitally (a), an example exhibiting that the vertical dual-beam pattern is deflected by the 2-bit coding pattern 01230123… (b), the meaning of addition theorme on the unit-cell level and metasurface-system level (c), and superposition of two dual-beam patterns achieved by the addition theorem (d)

(a) and (b) are reprinted from Liu S et al. (2016b), Copyright 2016, with permission from the authors, licensed under the Creative Commons Attribution; (c) and (d) are reprinted from Wu RY et al. (2018), Copyright 2018, with permission from WILEY-VCH Verlag GmbH & Co. KGaA, Weinheim

et al., 2016; Zheng et al., 2017; Shao et al., 2019). Moreover, vortex beams can be easily achieved using 3-bit coding metamaterials by arranging the coding particles with digits 0–7 in a clockwise or anticlockwise manner (Ma Q et al., 2017; Zhang L et al., 2017, Zheng et al., 2019). Furthermore, if the reflecting or transmitting amplitude is considered, the power of radiating beams can be tailored to also satisfy the various requirements for the targets at different locations in radar and communication systems (Bao et al., 2018).

All the coding schemes in the above-considered designs are periodic or quasi-periodic. When the coding particles are randomly arranged, the coding metamaterials can break up the incident EM waves into diffuse scattering patterns. This function enables the radar cross section (RCS) of coding metamaterials to reduce noticeably (Gao LH et al., 2015; Liang et al., 2015). For example, an elaborately designed Minkowski closed-loop coding particle is capable of generating 1-, 2-, and 3-bit digital states by tuning geometrical sizes in the terahertz band. By designing appropriate coding patterns, the random coding metasurfaces had strong ability to control the scattering terahertz waves, implying that the reflected terahertz energy was diffused across more directions (Gao LH et al., 2015). Vincenzo and his group (Moccia et al., 2017) introduced the Golay–Rudin–Shapiro (GRS) polynomial model into coding pattern design and achieved almost homogeneously anomalous reflection (Fig. 8). These digital approaches avoid the drawbacks of conventional manipulations of RCS, such as dependence on continual random phase contributions, which is hard to accomplish by computer and software.

In addition, the coding and digital concepts have been extended to surface-wave manipulations (Liu S et al., 2017, 2018). Liu S et al. (2017) proposed a 3-bit tensor coding metasurface to convert the propagating terahertz waves to surface waves. The working principle of this functionality can also be induced from Eq. (3). When the period of the coding sequence is smaller than the working wavelength, the outgoing waves cannot be radiated and are converted to surface

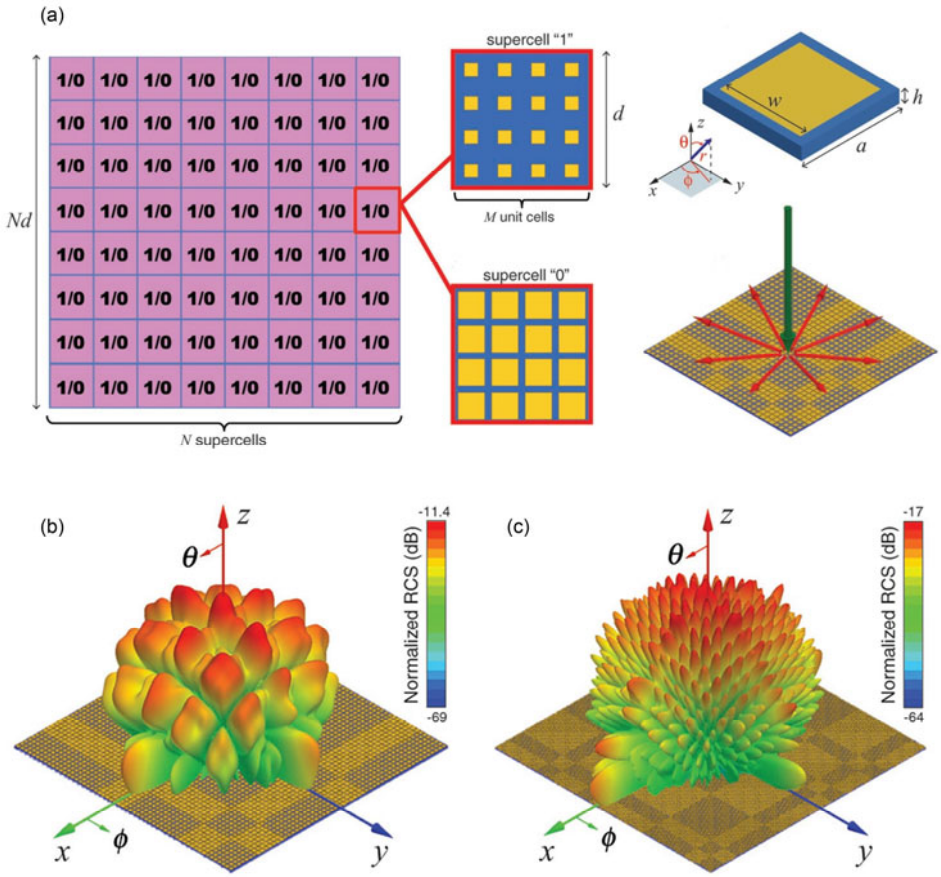

Fig. 8 Illustration of the radar cross section (RCS) reduction idea and geometry of the adopted particle (a) and the homogeneous RCS reduction inspired by the Golay–Rudin–Shapiro (GRS) polynomials (b, c)
Reprinted from Moccia et al. (2017), Copyright 2017, with permission from WILEY-VCH Verlag GmbH & Co. KGaA, Weinheim

waves. To ensure higher transformation efficiency, the period of the gradient coding sequence should be roughly equal to the working wavelength.

All above-mentioned coding and digital applications are limited in a single half space, e.g., the backward half space for reflection and the forward half space for transmission. Zhang L et al. (2018b) improved the available working region to the full space by controlling the EM property of *x*-polarized reflection, as well as the *y*-polarized transmission, on the two sides of the digital metasurface, independently. Furthermore, Wu RY et al. (2019) theoretically analyzed the working scheme of full-space radiating digital metasurface from the aspect of information science, where the forward and backward information can be manipulated independently (Fig. 9a). They further introduced the concept of 1-bit amplitude code characterized by full reflection and full transmission (Fig. 9b), which can enlarge the information capacity of the digital metasurface. The controls on amplitude codes depended on the polarization or active devices such as positive–intrinsic–negative (PIN) diodes. Combined with the traditional phase codes, the amplitude-phase controllable digital metamaterial can perform simultaneous or real-time shifting of full-space EM information manipulations (Fig. 9c) (Wu RY et al., 2019).

3.3 Novel systems based on programmable metamaterials

As discussed herein, the EM properties are efficiently expressed as several discrete digits in coding and digital metamaterials. This builds a bridge between information science and physical metamaterials,

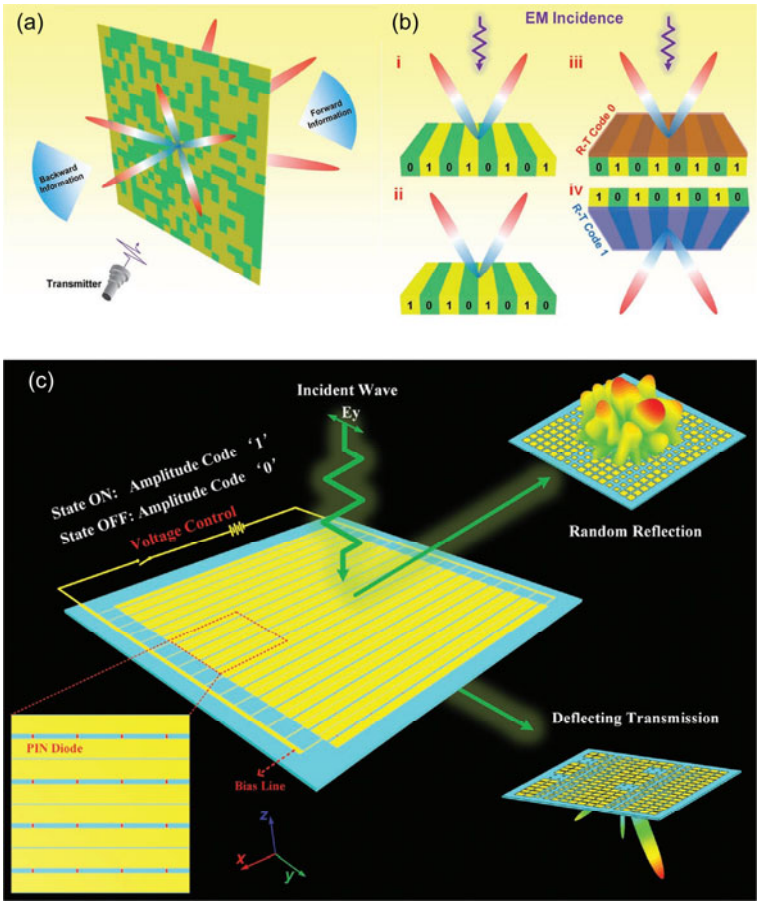

Fig. 9 Working scheme of the full-space radiating digital metasurface (the forward and backward information can be manipulated independently) (a), definition of the 1-bit amplitude code (digital states 0 and 1 represent total reflection and total transmission, respectively) (b), and graphical illustration of the digital metasurface with dynamic R–T amplitude code to achieve real-time full-space manipulations of EM information (c)

Reprinted from Wu RY et al. (2019), Copyright 2019, with permission from WILEY-VCH Verlag GmbH & Co. KGaA, Weinheim

also enabling the application of programmable controls on EM information in real time. Since digital information is involved in the metamaterials and we can achieve real-time manipulations on them, a grander concept of information metamaterial is established, including typical coding and digital theories and devices, as well as programmable designs and future information systems.

As the most basic programmable case, Cui et al. (2014) proposed an approach for constructing 1-bit programmable metamaterials by locating PIN diodes into the coding particles (Cui et al., 2014; Wan et al., 2016a). When the PIN diode is in the "ON" or "OFF" state, the digital states of the particle can be changed between "0" and "1" in real time. Moreover, we can use field-programmable gate array (FPGA) to transmit the digital information to the physical metamaterials (Fig. 10). When inputting different coding sequences by the triggers, the radiating pattern of the programmable metamaterial changes from single beam to multiple beams accordingly (Cui et al., 2014). If real-time control on digital states can be implemented on each particle independently, the radiations will show more types, such as four-beam pattern and diffusing scattering.

Adopting PIN diodes is not the only method for the real-time manipulation of digital states. Zhang XG et al. (2018) used light to control the voltage on the diodes, resulting in control of the digital states by rows. This approach possesses the remote manipulating property because the coding pattern is addressed and tuned by the illuminating light,

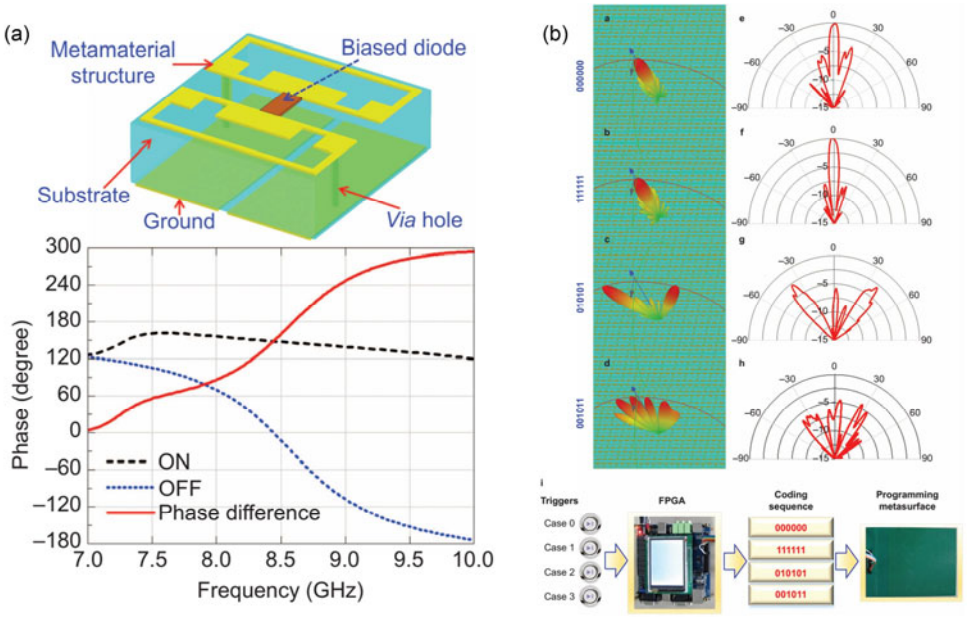

Fig. 10 Particle for programmable metamaterial and the 1-bit phase responses (a) and the real-time radiating-pattern manupulations by active devices and FPGA (b)

overcoming the complicated biasing wire network used to control each individual particle in the programmable metasurface.

Many novel systems using information metamaterials have been reported recently. Li YB et al. (2016b) adopted a 2-bit transmission-type programmable metasurface to achieve single-sensor and single-frequency target imaging in the microwave frequency. The programmable metasurface plays a very important role here to produce different real-time radiating patterns for single-sensor image reconstruction, avoiding object dispersion, compared with the other single-sensor imaging systems that use frequency agility. A holographic imaging system was proposed based on the 1-bit reflection-type programmable metasurface, as illustrated in Fig. 11a (Li LL et al., 2017). Multiple 1-bit digital holograms were formed by dynamically adjusting the voltages on each particle; thus, the metasurface hologram can successively project different holographic images. This research will be a key in enabling future intelligent metasurfaces with reconfigurable and programmable functionalities.

Cui et al. (2016) proposed the concept of information entropy of digital metamaterials. The Shannon information entropy was introduced to the metamaterial system, defining the geometric and physical information entropy of metamaterials and metasurfaces, with which the amount of information carried by the coding metamaterials and metasurfaces can be evaluated quantitatively. Because the information has been implanted in the coding patterns and corresponding digital metamaterials, we can acquire it from the near- or far-field radiating performances, respectively. Furthermore, Cui et al. (2019) proposed a novel communication system based only on information metamaterials, no longer restricted by the complex active/passive radio frequency (RF) devices. The only device was the 1-bit programmable coding particle that could convert the digital information to physical EM properties. This system has been demonstrated theoretically and experimentally. It provides a completely new architecture for wireless communications and may find promising applications in areas where information security is highly demanded. Moreover, Wan et al. (2019) established a near-field multichannel information transmitting system by converting the phase codes to amplitude codes in real time through 1-bit programmable metamaterials (Fig. 11b).

If the temporal dimension is taken into consideration (namely, the fact that the coding sequences are

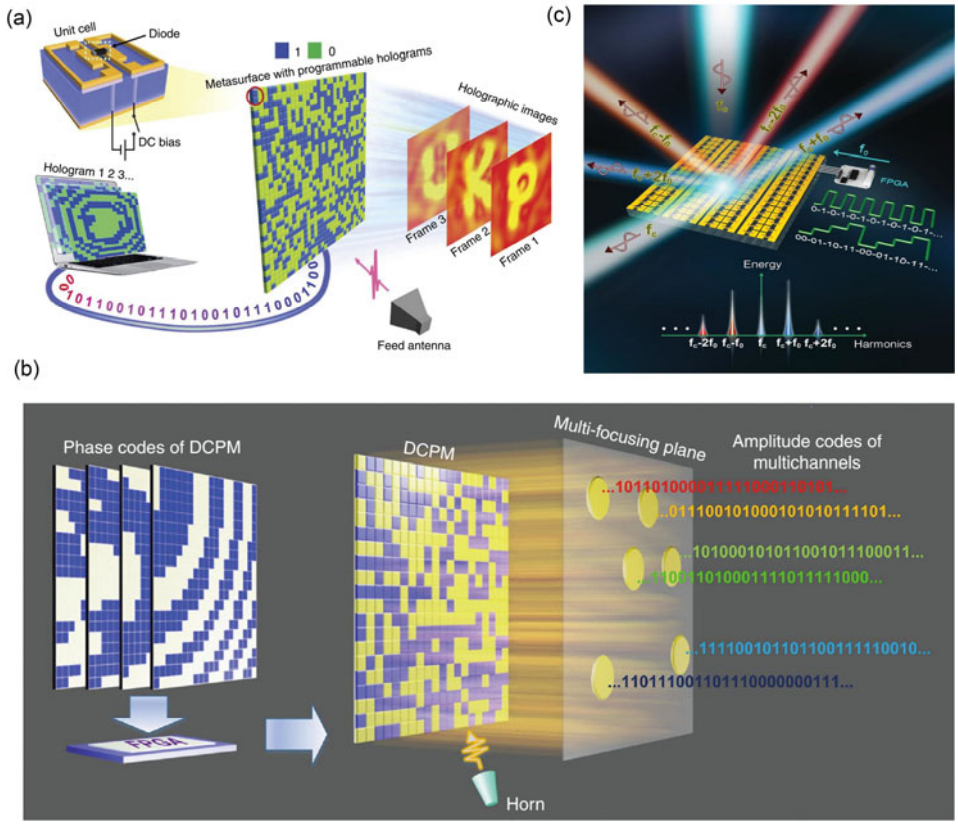

Fig. 11 Electromagnetic reprogrammable coding metasurface holograms (a), near-field multichannel information transmissions by converting the phase codes to amplitude codes (b), and novel information system by time-space coding metasurfaces (c)

(a) is reprinted from Li LL et al. (2017), Copyright 2017, with permission from Springer Nature, licensed under CC BY-4.0; (b) is reprinted from Wan et al. (2019), Copyright 2019, with permission from Springer Nature, licensed under CC BY-4.0; (c) is reprinted from Zhao et al. (2018), Copyright 2018, with permission from Oxford University Press, licensed under CC BY-4.0

now time-modulated), the programmable metamaterials are called space-time coding metamaterials. The amplitude and phase responses here are constructed by the time intervals controlled by the switches, which brings more interesting functionalities, such as non-linear harmonic manipulation and nonreciprocity, controlling the direction and amplitude of EM waves even in novel information systems (Fig. 11c) (Dai et al., 2018; Zhang L et al., 2018a, 2019; Zhao et al., 2018).

4 Conclusions and prospects

In conclusion, metamaterials have undergone overwhelming development in the past two decades, in both physical theory and actual engineering. We have reviewed them to give a global introduction from the initial effective medium metamaterials to the novel information metamaterials.

Metamaterials initially focused on controllable EM coefficients, such as permittivity and permeability, with the help of the effective medium theory. Elaborately arranged bulk meta-particles can show unnatural properties and induce EM waves to display exotic physics (e.g., invisibility cloaks, EM black holes, and EM tunneling effect); furthermore, several kinds of practical devices catering to engineering applications have been developed (e.g., GRIN lens for beam-steering antennas and high-resolution imaging).

Subsequently, metamaterials were also extended to the 2D case, namely, metasurfaces. Due to the geometrical difference in relation to metamaterials, analytical methods for metasurfaces usually rely on phase discontinuity according to the generalized Snell law, obviously decreasing the implementation complexity and difficulty. Using more efficient

meta-particles, metasurfaces have been adopted for various EM propagating phenomena coefficients, such as phase, amplitude, polarization, and frequency, and they have also been used in both spatial and surface wave manipulations. Compared with traditional metamaterials, metasurfaces have more integrating freedom in actual applications, corresponding to more interesting devices, including antennas, absorbers, and polarization converters. Furthermore, spoof SPPs emerged in the microwave region, with conformal and low-profile properties, opening a new branch of study due to their unusual advantages. They can support bizarre EM transmitting and radiating mechanisms that traditional microstrip lines cannot reach.

Currently, metamaterials and metasurfaces have developed to a newer stage, i.e., information metamaterials, building a bridge between the physical world and information science. Using the digital states, which can represent the various major EM properties such as phase and amplitude, EM information can be manipulated digitally, inspired by information theories. Hence, metamaterials are no longer the simple tools that transmit or receive information, but they constitutionally contain the corresponding digital information and enable novel applications such as digital beam-steering, diffused scattering, and other wavefront manipulations. More importantly, the highlight of information metamaterials is the amenability to programming and the real-time control of EM information. With the help of active devices located on meta-particles, programmable metamaterials can be adopted in real-time imaging, time-variable beam manipulation, and near- or far-field information control.

In the future, all the metamaterials mentioned in this review have the potential to achieve greater developments. Although effective-medium metamaterials have been widely investigated for more than 15 years, major research focuses on new physical phenomena. Hence, more attention should be paid to integrated, miniaturized, and low-cost metamaterials in engineering. For metasurfaces, exploring multi-coefficient and multi-functional metasurfaces with higher efficiency should be focused on. For spoof SPPs, on-chip SPP devices should be further considered to achieve SPP-based information systems. Using compact SPP devices can efficiently reduce the volume and complexity of microwave systems and even achieve full-SPP systems. For information metamaterials, the combination with information science must be the main developing trend. First, we should propose original and meaningful methods and operations on coding patterns. Next, we can extend programmable metamaterials to more advanced intelligent metamaterials and software-driven metamaterials inspired by artificial intelligence and deep learning. Finally, information metamaterials can lead to more real-time digital manipulations of EM waves, even novel information communication and processing systems.

Contributors

Rui-yuan WU wrote the first draft of the manuscript. Tie-jun CUI helped organize the manuscript. Rui-yuan WU and Tie-jun CUI revised and edited the final version.

Compliance with ethics guidelines

Rui-yuan WU and Tie-jun CUI declare that they have no conflict of interest.

References

Bai GD, Ma Q, Iqbal S, et al., 2018. Multitasking shared aperture enabled with multiband digital coding metasurface. *Adv Opt Mater*, 6(21):1800657. https://doi.org/10.1002/adom.201800657

Bai GD, Ma Q, Cao WK, et al., 2019. Manipulation of electromagnetic and acoustic wave behaviors via shared digital coding metallic metasurface. *Adv Intell Syst*, 1(5): 1900038. https://doi.org/10.1002/aisy.201900038

Bao L, Ma Q, Bai GD, et al., 2018. Design of digital coding metasurfaces with independent controls of phase and amplitude responses. *Appl Phys Lett*, 113(6):063502. https://doi.org/10.1063/1.5043520

Bie X, Jing XF, Hong Z, et al., 2018. Flexible control of transmitting terahertz beams based on multilayer encoding metasurfaces. *Appl Opt*, 57(30):9070-9077. https://doi.org/10.1364/AO.57.009070

Cai BG, Li YB, Jiang WX, et al., 2015. Generation of spatial Bessel beams using holographic metasurface. *Opt Expr*, 23(6):7593-7601. https://doi.org/10.1364/OE.23.007593

Chen HS, Wu BI, Zhang BL, et al., 2007. Electromagnetic wave interactions with a metamaterial cloak. *Phys Rev Lett*, 99(6):063903. https://doi.org/10.1103/PhysRevLett.99.063903

Chen HT, Taylor AJ, Yu NF, 2016. A review of metasurfaces: physics and applications. *Rep Progr Phys*, 79(7):076401. https://doi.org/10.1088/0034-4885/79/7/076401

Chen K, Feng YJ, Monticone F, et al., 2017. A reconfigurable active Huygens' metalens. *Adv Mater*, 29(17):1606422.

https://doi.org/10.1002/adma.201606422

Chen MLN, Jiang LJ, Sha W, 2016. Ultrathin complementary metasurface for orbital angular momentum generation at microwave frequencies. *IEEE Trans Antenn Propag*, 65(1):396-400. https://doi.org/10.1109/TAP.2016.2626722

Chen X, Ma HF, Zou XY, et al., 2011. Three-dimensional broadband and high-directivity lens antenna made of metamaterials. *J Appl Phys*, 110(4):044904. https://doi.org/10.1063/1.3622596

Cheng Q, Cui TJ, Jiang WX, et al., 2010. An omnidirectional electromagnetic absorber made of metamaterials. *New J Phys*, 12(6):063006. https://doi.org/10.1088/1367-2630/12/6/063006

Collin RE, 1960. Field Theory of Guided Waves. McGraw-Hill, New York.

Cui TJ, 2017. Microwave metamaterials—from passive to digital and programmable controls of electromagnetic waves. *J Opt*, 19(8):084004. https://doi.org/10.1088/2040-8986/aa7009

Cui TJ, 2018. Microwave metamaterials. *Nat Sci Rev*, 5(2): 134-136. https://doi.org/10.1093/nsr/nwx133

Cui TJ, Smith DR, Liu R, 2010. Metamaterials: Theory, Design, and Applications. Springer, New York.

Cui TJ, Qi MQ, Wan X, et al., 2014. Coding metamaterials, digital metamaterials and programmable metamaterials. *Light Sci Appl*, 3(10):e218. https://doi.org/10.1038/lsa.2014.99

Cui TJ, Liu S, Li LL, 2016. Information entropy of coding metasurface. *Light Sci Appl*, 5(11):e16172. https://doi.org/10.1038/lsa.2016.172

Cui TJ, Liu S, Zhang L, 2017a. Information metamaterials and metasurfaces. *J Mater Chem C*, 5(15):3644-3668. https://doi.org/10.1039/C7TC00548B

Cui TJ, Wu RY, Wu W, et al., 2017b. Large-scale transmission-type multifunctional anisotropic coding metasurfaces in millimeter-wave frequencies. *J Phys D*, 50(40):404002. https://doi.org/10.1088/1361-6463/aa85bd

Cui TJ, Liu S, Bai GD, et al., 2019. Direct transmission of digital message via programmable coding metasurface. *Research*, 2019:2584509. https://doi.org/10.34133/2019/2584509

Dai JY, Zhao J, Cheng Q, et al., 2018. Independent control of harmonic amplitudes and phases via a time-domain digital coding metasurface. *Light Sci Appl*, 7(1):90. https://doi.org/10.1038/s41377-018-0092-z

Ding F, Pors A, Bozhevolnyi SI, 2017. Gradient metasurfaces: a review of fundamentals and applications. *Rep Progr Phys*, 81(2):026401. https://doi.org/10.1088/1361-6633/aa8732

Engheta N, Ziolkowski RW, 2006. Electromagnetic Metamaterials: Physics and Engineering Explorations. Wiley and IEEE Press, Hoboken.

Fu XJ, Cui TJ, 2019. Recent progress on metamaterials: from effective medium model to real-time information processing system. *Progr Quant Electron*, 67:100223. https://doi.org/10.1016/j.pquantelec.2019.05.001

Gao LH, Cheng Q, Yang J, et al., 2015. Broadband diffusion of terahertz waves by multi-bit coding metasurfaces. *Light Sci Appl*, 4(9):e324. https://doi.org/10.1038/lsa.2015.97

Gao X, Han X, Cao WP, et al., 2015. Ultrawideband and high-efficiency linear polarization converter based on double V-shaped metasurface. *IEEE Trans Antenn Propag*, 63(8):3522-3530. https://doi.org/10.1109/TAP.2015.2434392

Gao Z, Wu L, Gao F, et al., 2018. Spoof plasmonics: from metamaterial concept to topological description. *Adv Mater*, 30(31):1706683. https://doi.org/10.1002/adma.201706683

Garcia-Vidal J, Martín-Moreno L, Pendry JB, 2005. Surfaces with holes in them: new plasmonic metamaterials. *J Opt A*, 7(2):S97-S101. https://doi.org/10.1088/1464-4258/7/2/013

Gil M, Bonache J, Martín F, 2008. Metamaterial filters: a review. *Metamaterials*, 2(4):186-197. https://doi.org/10.1016/j.metmat.2008.07.006

Giovampaola CD, Engheta N, 2014. Digital metamaterials. *Nat Mater*, 13(12):1115-1121. https://doi.org/10.1038/nmat4082

Han JQ, Li L, Yi H, et al., 2018. 1-bit digital orbital angular momentum vortex beam generator based on a coding reflective metasurface. *Opt Mater Expr*, 8(11):3470-3478. https://doi.org/10.1364/OME.8.003470

Holloway CL, Kuester EF, Gordon JA, et al., 2012. An overview of the theory and applications of metasurfaces: the two-dimensional equivalents of metamaterials. *IEEE Antenn Propag Mag*, 54(2):10-35. https://doi.org/10.1109/MAP.2012.6230714

Huang YJ, Wen GJ, Li J, et al., 2013. Wide-angle and polarization-independent metamaterial absorber based on snowflake-shaped configuration. *J Electromagn Waves Appl*, 27(5):552-559. https://doi.org/10.1080/09205071.2013.756383

Jiang WX, Ge S, Han TC, et al., 2016. Shaping 3D path of electromagnetic waves using gradient-refractive-index metamaterials. *Adv Sci*, 3(8):1600022. https://doi.org/10.1002/advs.201600022

Jing Y, Li YF, Zhang JQ, et al., 2018. Fast coding method of metasurfaces based on 1D coding in orthogonal directions. *J Phys D*, 51(47):475103. https://doi.org/10.1088/1361-6463/aae2fd

Karimi E, Schulz SA, de Leon I, et al., 2014. Generating optical orbital angular momentum at visible wavelengths using a plasmonic metasurface. *Light Sci Appl*, 3(5): e167. https://doi.org/10.1038/lsa.2014.48

Kong GS, Ma HF, Cai BG, et al., 2016. Continuous leaky-wave scanning using periodically modulated spoof plasmonic waveguide. *Sci Rep*, 6:29600. https://doi.org/10.1038/srep29600

Kuester EF, Mohamed MA, Piket-May M, et al., 2003. Averaged transition conditions for electromagnetic fields at a metafilm. *IEEE Trans Antenn Propag*, 51(10):2641- 2651.

https://doi.org/10.1109/TAP.2003.817560

Kundtz N, Smith DR, 2010. Extreme-angle broadband metamaterial lens. *Nat Mater*, 9(2):129-132. https://doi.org/10.1038/NMAT2610

Landy N, Smith DR, 2013. A full-parameter unidirectional metamaterial cloak for microwaves. *Nat Mater*, 12(1): 25-28. https://doi.org/10.1038/NMAT3476

Li HP, Wang GM, Gao XJ, et al., 2018. A novel metasurface for dual-mode and dual-band flat high-gain antenna application. *IEEE Trans Antenn Propag*, 66(7):3706-3711. https://doi.org/10.1109/TAP.2018.2835526

Li K, Li L, Cai YM, et al., 2015. A novel design of low-profile dual-band circularly polarized antenna with meta-surface. *IEEE Antenn Wirel Propag Lett*, 14:1650-1653. https://doi.org/10.1109/LAWP.2015.2417169

Li LL, Cui TJ, 2019. Information metamaterials—from effective media to real-time information processing systems. *Nanophotonics*, 8(5):703-724. https://doi.org/10.1515/nanoph-2019-0006

Li LL, Cui TJ, Ji W, et al., 2017. Electromagnetic reprogrammable coding-metasurface holograms. *Nat Commun*, 8(1):197. https://doi.org/10.1038/s41467-017-00164-9

Li Y, Assouar BM, 2016. Acoustic metasurface-based perfect absorber with deep subwavelength thickness. *Appl Phys Lett*, 108(6):063502. https://doi.org/10.1063/1.4941338

Li Y, Liang B, Gu ZM, et al., 2013. Reflected wavefront manipulation based on ultrathin planar acoustic metasurfaces. *Sci Rep*, 3:2546. https://doi.org/10.1038/srep02546

Li YB, Wan X, Cai BG, et al., 2014. Frequency-controls of electromagnetic multi-beam scanning by metasurfaces. *Sci Rep*, 4:6921. https://doi.org/10.1038/srep06921

Li YB, Cai BG, Cheng Q, et al., 2016a. Isotropic holographic metasurfaces for dual-functional radiations without mutual interferences. *Adv Funct Mater*, 26(1):29-35. https://doi.org/10.1002/adfm.201503654

Li YB, Li LL, Xu BB, et al., 2016b. Transmission-type 2-bit programmable metasurface for single-sensor and single-frequency microwave imaging. *Sci Rep*, 6:23731. https://doi.org/10.1038/srep23731

Li ZC, Liu WW, Cheng H, et al., 2015. Realizing broadband and invertible linear-to-circular polarization converter with ultrathin single-layer metasurface. *Sci Rep*, 5:18106. https://doi.org/10.1038/srep18106

Li ZC, Liu WW, Cheng H, et al., 2016. Tunable dual-band asymmetric transmission for circularly polarized waves with graphene planar chiral metasurfaces. *Opt Lett*, 41(13): 3142-3145. https://doi.org/10.1364/OL.41.003142

Liang LJ, Qi MQ, Yang J, et al., 2015. Anomalous terahertz reflection and scattering by flexible and conformal coding metamaterials. *Adv Opt Mater*, 3(10):1374-1380. https://doi.org/10.1002/adom.201500206

Liao Z, Zhao J, Pan BC, et al., 2014. Broadband transition between microstrip line and conformal surface plasmon waveguide. *J Phys D*, 47(31):315103. https://doi.org/10.1088/0022-3727/47/31/315103

Lin XQ, Cui TJ, Chin JY, et al., 2008. Controlling electromagnetic waves using tunable gradient dielectric metamaterial lens. *Appl Phys Lett*, 92(13):131904. https://doi.org/10.1063/1.2896308

Liu LX, Zhang XQ, Kenney M, et al., 2014. Broadband metasurfaces with simultaneous control of phase and amplitude. *Adv Mater*, 26(29):5031-5036. https://doi.org/10.1002/adma.201401484

Liu R, Ji C, Mock JJ, et al., 2009. Broadband ground-plane cloak. *Science*, 323(5912):366-369. https://doi.org/10.1126/science.1166949

Liu RP, Cui TJ, Huang D, et al., 2007. Description and explanation of electromagnetic behaviors in artificial metamaterials based on effective medium theory. *Phys Rev E*, 76(2):026606. https://doi.org/10.1103/PhysRevE.76.026606

Liu S, Chen HB, Cui TJ, 2015. A broadband terahertz absorber using multi-layer stacked bars. *Appl Phys Lett*, 106(15): 151601. https://doi.org/10.1063/1.4918289

Liu S, Cui TJ, Xu Q, et al., 2016a. Anisotropic coding metamaterials and their powerful manipulation of differently polarized terahertz waves. *Light Sci Appl*, 5(5):e16076. https://doi.org/10.1038/lsa.2016.76

Liu S, Cui TJ, Zhang L, et al., 2016b. Convolution operations on coding metasurface to reach flexible and continuous controls of terahertz beams. *Adv Sci*, 3(10):1600156. https://doi.org/10.1002/advs.201600156

Liu S, Zhang L, Yang QL, et al., 2016c. Frequency-dependent dual-functional coding metasurfaces at terahertz frequencies. *Adv Opt Mater*, 4(12):1965-1973. https://doi.org/10.1002/adom.201600471

Liu S, Zhang HC, Zhang L, et al., 2017. Full-state controls of terahertz waves using tensor coding metasurfaces. *ACS Appl Mater Interf*, 9(25):21503-21514. https://doi.org/10.1021/acsami.7b02789

Liu S, Cui TJ, Noor A, et al., 2018. Negative reflection and negative surface wave conversion from obliquely incident electromagnetic waves. *Light Sci Appl*, 7(5):18008. https://doi.org/10.1038/lsa.2018.8

Liu XY, Feng YJ, Zhu B, et al., 2016. Backward spoof surface wave in plasmonic metamaterial of ultrathin metallic structure. *Sci Rep*, 6:20448. https://doi.org/10.1038/srep20448

Ma HF, Cui TJ, 2010a. Three-dimensional broadband ground-plane cloak made of metamaterials. *Nat Commun*, 1(1):21. https://doi.org/10.1038/ncomms1023

Ma HF, Cui TJ, 2010b. Three-dimensional broadband and broad-angle transformation-optics lens. *Nat Commun*, 1(1):124. https://doi.org/10.1038/ncomms1126

Ma HF, Shen XP, Cheng Q, et al., 2014. Broadband and high-efficiency conversion from guided waves to spoof surface plasmon polaritons. *Laser Photon Rev*, 8(1): 146-151. https://doi.org/10.1002/lpor.201300118

Ma Q, Shi CB, Bai GD, et al., 2017. Beam-editing coding metasurfaces based on polarization bit and orbital-angular-momentum-mode bit. *Adv Opt Mater*, 5(23): 1700548. https://doi.org/10.1002/adom.201700548

Markovich DL, Andryieuski A, Zalkovskij M, et al., 2013. Metamaterial polarization converter analysis: limits of performance. *Appl Phys B*, 112(2):143-152. https://doi.org/10.1007/s00340-013-5383-8

Minatti G, Maci S, de Vita P, et al., 2012. A circularly-polarized isoflux antenna based on anisotropic metasurface. *IEEE Trans Antenn Propag*, 60(11):4998-5009. https://doi.org/10.1109/TAP.2012.2208614

Moccia M, Liu S, Wu RY, et al., 2017. Coding metasurfaces for diffuse scattering: scaling laws, bounds, and suboptimal design. *Adv Opt Mater*, 5(19):1700455. https://doi.org/10.1002/adom.201700455

Moitra P, Yang YM, Anderson Z, et al., 2013. Realization of an all-dielectric zero-index optical metamaterial. *Nat Photon*, 7(10):791-795. https://doi.org/10.1038/nphoton.2013.214

Narimanov EE, Kildishev AV, 2009. Optical black hole: broadband omnidirectional light absorber. *Appl Phys Lett*, 95(4):041106. https://doi.org/10.1063/1.3184594

O'Hara JF, Averitt RD, Taylor AJ, 2005. Prism coupling to terahertz surface plasmon polaritons. *Opt Expr*, 13(16): 6117-6126. https://doi.org/10.1364/OPEX.13.006117

Padilla WJ, Basov DN, Smith DR, 2006. Negative refractive index metamaterials. *Mater Today*, 9(7-8):28-35. https://doi.org/10.1016/S1369-7021(06)71573-5

Park J, Youn JR, Song YS, 2019. Hydrodynamic metamaterial cloak for drag-free flow. *Phys Rev Lett*, 123(7):074502. https://doi.org/10.1103/PhysRevLett.123.074502

Pendry JB, 2000. Negative refraction makes a perfect lens. *Phys Rev Lett*, 85(18):3966-3969. https://doi.org/10.1103/PhysRevLett.85.3966

Pendry JB, Holden AJ, Stewart WJ, et al., 1996. Extremely low frequency plasmons in metallic mesostructures. *Phys Rev Lett*, 76(25):4773-4776. https://doi.org/10.1103/PhysRevLett.76.4773

Pendry JB, Holden AJ, Robbins DJ, et al., 1999. Magnetism from conductors and enhanced nonlinear phenomena,. *IEEE Trans Microw Theory Techn*, 47(11):2075-2084. https://doi.org/10.1109/22.798002

Pendry JB, Martín-Moreno L, Garcia-Vidal FJ, 2004. Mimicking surface plasmons with structured surfaces. *Science*, 305(5685):847-848. https://doi.org/10.1126/science.1098999

Pendry JB, Schurig D, Smith DR, 2006. Controlling electromagnetic fields. *Science*, 312(5781):1780-1782. https://doi.org/10.1126/science.1125907

Pfeiffer C, Grbic A, 2013. Metamaterial Huygens' surfaces: tailoring wave fronts with reflectionless sheets. *Phys Rev Lett*, 110(19):197401. https://doi.org/10.1103/PhysRevLett.110.197401

Qi MQ, Tang WX, Xu HX, et al., 2013. Tailoring radiation patterns in broadband with controllable aperture field using metamaterials. *IEEE Trans Antenn Propag*, 61(11):5792-5798. https://doi.org/10.1109/TAP.2013.2276921

Ramaccia D, Scattone F, Bilotti F, et al., 2013. Broadband compact horn antennas by using EPS-ENZ metamaterial lens. *IEEE Trans Antenn Propag*, 61(6):2929-2937. https://doi.org/10.1109/TAP.2013.2250235

Schurig D, Mock JJ, Justice BJ, et al., 2006. Metamaterial electromagnetic cloak at microwave frequencies. *Science*, 314(5801):977-980. https://doi.org/10.1126/science.1133628

Shalaev MI, Sun JB, Tsukernik A, et al., 2015. High-efficiency all-dielectric metasurfaces for ultracompact beam manipulation in transmission mode. *Nano Lett*, 15(9):6261-6266. https://doi.org/10.1021/acs.nanolett.5b02926

Shao LD, Zhu WR, Leonov MY, et al., 2019. Dielectric 2-bit coding metasurface for electromagnetic wave manipulation. *J Appl Phys*, 125(20):203101. https://doi.org/10.1063/1.5094561

Shelby RA, Smith DR, Schultz S, 2001. Experimental verification of a negative index of refraction. *Science*, 292(5514):77-79. https://doi.org/10.1126/science.1058847

Shen XP, Cui TJ, 2013. Planar plasmonic metamaterial on a thin film with nearly zero thickness. *Appl Phys Lett*, 102(21):211909. https://doi.org/10.1063/1.4808350

Shen XP, Cui TJ, Martin-Cano D, et al., 2013. Conformal surface plasmons propagating on ultrathin and flexible films. *Proc Nat Acad Sci USA*, 110(1):40-45. https://doi.org/10.1073/pnas.1210417110

Shen Z, Jin BB, Zhao JM, et al., 2016. Design of transmission-type coding metasurface and its application of beam forming. *Appl Phys Lett*, 109(12):121103. https://doi.org/10.1063/1.4962947

Sievenpiper D, Zhang LJ, Broas RFJ, et al., 1999. High-impedance electromagnetic surfaces with a forbidden frequency band. *IEEE Trans Microw Theory Techn*, 47(11):2059-2074. https://doi.org/10.1109/22.798001

Smith DR, Padilla WJ, Vier DC, et al., 2000. Composite medium with simultaneously negative permeability and permittivity. *Phys Rev Lett*, 84(18):4184-4187. https://doi.org/10.1103/PhysRevLett.84.4184

Smith DR, Pendry JB, Wiltshire MCK, 2004. Metamaterials and negative refractive index. *Science*, 305(5685): 788-792. https://doi.org/10.1126/science.1096796

Sun JB, Liu LY, Dong GY, et al., 2011. An extremely broad band metamaterial absorber based on destructive interference. *Opt Expr*, 19(22):21155-21162. https://doi.org/10.1364/OE.19.021155

Sun SL, He Q, Xiao SY, et al., 2012. Gradient-index metasurfaces as a bridge linking propagating waves and surface waves. *Nat Mater*, 11(5):426-431. https://doi.org/10.1038/nmat3292

Tang WX, Zhang HC, Ma HF, et al., 2019. Concept, theory, design, and applications of spoof surface plasmon polaritons at microwave frequencies. *Adv Opt Mater*, 7(1): 1800421. https://doi.org/10.1002/adom.201800421

Veselago VG, 1967. Electrodynamics of substances with simultaneously negative values of ε and μ. *Usp Fiz Nauk*, 92:517-526.

Wakatsuchi H, Kim S, Rushton JJ, et al., 2013. Waveform-dependent absorbing metasurfaces. *Phys Rev Lett*, 111(24):245501. https://doi.org/10.1103/PhysRevLett.111.245501

Wan X, Shen XP, Luo Y, et al., 2014. Planar bifunctional Luneburg-fisheye lens made of an anisotropic metasurface. *Laser Photon Rev*, 8(5):757-765. https://doi.org/10.1002/lpor.201400023

Wan X, Qi MQ, Chen TY, et al., 2016a. Field-programmable beam reconfiguring based on digitally-controlled coding metasurface. *Sci Rep*, 6:20663. https://doi.org/10.1038/srep20663

Wan X, Jia SL, Cui TJ, et al., 2016b. Independent modulations of the transmission amplitudes and phases by using Huygens metasurfaces. *Sci Rep*, 6:25639. https://doi.org/10.1038/srep25639

Wan X, Zhang Q, Chen TY, et al., 2019. Multichannel direct transmissions of near-field information. *Light Sci Appl*, 8(1):60. https://doi.org/10.1038/s41377-019-0169-3

Wang M, Ma HF, Zhang HC, et al., 2018. Frequency-fixed beam-scanning leaky-wave antenna using electronically controllable corrugated microstrip line. *IEEE Trans Antenn Propag*, 66(9):4449-4457. https://doi.org/10.1109/TAP.2018.2845452

Wang ZX, Zhang HC, Lu J, et al., 2018. Compact filters with adjustable multi-band rejections based on spoof surface plasmon polaritons. *J Phys D*, 52(2):025107. https://doi.org/10.1088/1361-6463/aae885

Wei ZY, Cao Y, Su XP, et al., 2013. Highly efficient beam steering with a transparent metasurface. *Opt Expr*, 21(9): 10739-10745. https://doi.org/10.1364/OE.21.010739

Wong AMH, Eleftheriades GV, 2018. Perfect anomalous reflection with a bipartite Huygens' metasurface. *Phys Rev X*, 8(1):011036. https://doi.org/10.1103/PhysRevX.8.011036

Wu HT, Liu S, Wan X, et al., 2017. Controlling energy radiations of electromagnetic waves via frequency coding metamaterials. *Adv Sci*, 4(9):1700098. https://doi.org/10.1002/advs.201700098

Wu PC, Zhu WM, Shen ZX, et al., 2017. Broadband wide-angle multifunctional polarization converter via liquid-metal-based metasurface. *Adv Opt Mater*, 5(7): 1600938. https://doi.org/10.1002/adom.201600938

Wu RY, Shi CB, Liu S, et al., 2018. Addition theorem for digital coding metamaterials. *Adv Opt Mater*, 6(5): 1701236. https://doi.org/10.1002/adom.201701236

Wu RY, Zhang L, Bao L, et al., 2019. Digital metasurface with phase code and reflection-transmission amplitude code for flexible full-space electromagnetic manipulations. *Adv Opt Mater*, 7(8):1801429. https://doi.org/10.1002/adom.201801429

Xie BY, Tang K, Cheng H, et al., 2017. Coding acoustic metasurfaces. *Adv Mater*, 29(6):1603507. https://doi.org/10.1002/adma.201603507

Xu HX, Hu GW, Han L, et al., 2019. Chirality-assisted high-efficiency metasurfaces with independent control of phase, amplitude, and polarization. *Adv Opt Mater*, 7(4): 1801479. https://doi.org/10.1002/adom.201801479

Xu J, Li RQ, Wang SY, et al., 2018. Ultra-broadband linear polarization converter based on anisotropic metasurface. *Opt Expr*, 26(20):26235-26241. https://doi.org/10.1364/OE.26.026235

Yi XN, Ling XH, Zhang ZY, et al., 2014. Generation of cylindrical vector vortex beams by two cascaded metasurfaces. *Opt Expr*, 22(14):17207-17215. https://doi.org/10.1364/OE.22.017207

Yin JY, Ren J, Zhang Q, et al., 2016. Frequency-controlled broad-angle beam scanning of patch array fed by spoof surface plasmon polaritons. *IEEE Trans Antenn Propag*, 64(12):5181-5189. https://doi.org/10.1109/TAP.2016.2623663

Yu NF, Genevet P, Kats MA, et al., 2012. Light propagation with phase discontinuities: generalized laws of reflection and refraction. *Science*, 334(6504):333-337. https://doi.org/10.1126/science.1210713

Yu SX, Li L, Shi GM, et al., 2016a. Design, fabrication, and measurement of reflective metasurface for orbital angular momentum vortex wave in radio frequency domain. *Appl Phys Lett*, 108(12):121903. https://doi.org/10.1063/1.4944789

Yu SX, Li L, Shi GM, 2016b. Dual-polarization and dual-mode orbital angular momentum radio vortex beam generated by using reflective metasurface. *Appl Phys Expr*, 9(8):082202. https://doi.org/10.7567/APEX.9.082202

Yu SX, Li L, Shi GM, et al., 2016c. Generating multiple orbital angular momentum vortex beams using a metasurface in radio frequency domain. *Appl Phys Lett*, 108(24):241901. https://doi.org/10.1063/1.4953786

Zhang C, Cao WK, Yang J, et al., 2019. Multiphysical digital coding metamaterials for independent control of broadband electromagnetic and acoustic waves with a large variety of functions. *ACS Appl Mater Interf*, 11(18): 17050-17055. https://doi.org/10.1021/acsami.9b02490

Zhang HC, Liu S, Shen XP, et al., 2015a. Broadband amplification of spoof surface plasmon polaritons at microwave frequencies. *Laser Photon Rev*, 9(1):83-90. https://doi.org/10.1002/lpor.201400131

Zhang HC, Fan YF, Guo J, et al., 2015b. Second-harmonic generation of spoof surface plasmon polaritons using nonlinear plasmonic metamaterials. *ACS Photon*, 3(1): 139-146. https://doi.org/10.1021/acsphotonics.5b00580

Zhang L, Mei ST, Huang K, et al., 2016. Advances in full control of electromagnetic waves with metasurfaces. *Adv Opt Mater*, 4(6):818-833. https://doi.org/10.1002/adom.201500690

Zhang L, Liu S, Li LL, et al., 2017. Spin-controlled multiple pencil beams and vortex beams with different polarizations generated by Pancharatnam-Berry coding metasurfaces. *ACS Appl Mater Interf*, 9(41):36447-36455.

https://doi.org/10.1021/acsami.7b12468

Zhang L, Chen XQ, Liu S, et al., 2018a. Space-time-coding digital metasurfaces. *Nat Commun*, 9:4334. https://doi.org/10.1038/s41467-018-06802-0

Zhang L, Wu RY, Bai GD, et al., 2018b. Transmission-reflection-integrated multifunctional coding metasurface for full-space controls of electromagnetic waves. *Adv Funct Mater*, 28(33):1802205. https://doi.org/10.1002/adfm.201802205

Zhang L, Chen XQ, Shao RW, et al., 2019. Breaking reciprocity with space-time-coding digital metasurfaces. *Adv Mater*, 31(41):1904069. https://doi.org/10.1002/adma.201904069

Zhang Q, Zhang HC, Yin JY, et al., 2016. A series of compact rejection filters based on the interaction between spoof SPPs and CSRRs. *Sci Rep*, 6:28256. https://doi.org/10.1038/srep28256

Zhang Q, Wan X, Liu S, et al., 2017. Shaping electromagnetic waves using software-automatically-designed metasurfaces. *Sci Rep*, 7:3588. https://doi.org/10.1038/s41598-017-03764-z

Zhang Q, Liu C, Wan X, et al., 2019. Machine-learning designs of anisotropic digital coding metasurfaces. *Adv Theory Simul*, 2(2):1800132. https://doi.org/10.1002/adts.201800132

Zhang XG, Tang WX, Jiang WX, et al., 2018. Light—controllable digital coding metasurfaces. *Adv Sci*, 5(11): 1870068. https://doi.org/10.1002/advs.201801028

Zhang XR, Tang WX, Zhang HC, et al., 2018. A spoof surface plasmon transmission line loaded with varactors and short-circuit stubs and its application in Wilkinson power dividers. *Adv Mater Technol*, 3(6):1800046. https://doi.org/10.1002/admt.201800046

Zhao J, Cheng Q, Chen J, et al., 2013. A tunable metamaterial absorber using varactor diodes. *New J Phys*, 15(4): 043049. https://doi.org/10.1088/1367-2630/15/4/043049

Zhao J, Yang X, Dai JY, et al., 2018. Programmable time-domain digital-coding metasurface for non-linear harmonic manipulation and new wireless communication systems. *Nat Sci Rev*, 6(2):231-238. https://doi.org/10.1093/nsr/nwy135

Zheludev NI, Kivshar YS, 2012. From metamaterials to metadevices. *Nat Mater*, 11(11):917-924. https://doi.org/10.1038/NMAT3431

Zheng QQ, Li YF, Zhang JQ, et al., 2017. Wideband, wide-angle coding phase gradient metasurfaces based on Pancharatnam-Berry phase. *Sci Rep*, 7:43543. https://doi.org/10.1038/srep43543

Zheng QQ, Li YF, Han YJ, et al., 2019. Efficient orbital angular momentum vortex beam generation by generalized coding metasurface. *Appl Phys A*, 125(2):136. https://doi.org/10.1007/s00339-018-2373-z